Appendix G: GPR Methods Investigation Report

This appendix contains the full, detailed report of the findings of the GPR methods investigation (Sturm 2010).

Report on Ground-Penetrating Radar Surveys Method Investigation

Honolulu High-Capacity Transit Corridor Project (HHCTCP)

December 6, 2010

Submitted to:

Matt McDermott
Cultural Surveys Hawaii, Inc.
P.O. Box 1114
Kailua, HI 96734

Submitted by:

Jennie O. Sturm, M.A.
TAG Research by Sturm Inc.
550 Goliad Ct. NW
Albuquerque, NM 87107
303-349-1101
jsturm@tagrsi.com

Table of Contents

Executive Summary

This report presents the findings and assessment of the ground-penetrating radar (GPR) surveys conducted in select areas for the Honolulu High-Capacity Transit Corridor Project (HHCTCP) in downtown Honolulu, Hawaii. Six areas were chosen for surveying with three different antenna frequencies (270 MHz, 400 MHz, and 900 MHz) in consultation with Matt McDermott of Cultural Surveys Hawaii, Inc., to test a range of target features and settings. These included areas with known burials, areas with hypothesized burials, areas with utilities, and areas with asphalt and concrete paving. In several of the areas, all three antenna frequencies were able to map the features of interest, though with varying degrees of resolution. In general, the 400 MHz antenna provided the best overall quality data, allowing high resolution mapping of target features of interest (including burials) to a depth of approximately 1 to 1.5 meters.

Introduction

The purpose of this project was to use ground-penetrating radar (GPR) surveys in select areas within the downtown Honolulu setting to test this method's efficacy in mapping cultural features of interest. There are a number of archaeologically sensitive areas within the downtown Honolulu area, and so it was important to assess whether or not features of potential interest could be located and mapped in a non-invasive way. The high resolution mapping capabilities and depth information provided by the GPR method makes this the most promising geophysical technique for imaging the cultural features of interest, and especially human burials. In addition, GPR is the only geophysical method that is not irreparably affected by asphalt, surface metal objects, power lines, and other typical urban features, making it especially pertinent in the downtown Honolulu setting. Previous GPR surveys conducted in nearby locations had demonstrated the potential of this method to map the stratigraphy and buried features in this area, though overall depth penetration and feature resolution remained a concern (Matt McDermott, personal communication). This project therefore sought to evaluate and test which antenna frequencies, collection parameters, and processing procedures would be the most effective for potentially mapping and identifying the cultural features of interest within this setting.

The current investigation involved GPR surveys at six locations: the Alapai Transit Center, St. Augustine Church, a portion of Halekauwila Street, the proposed location of the Civic Center Transit Station, and two areas at the Kaka‘ako Fire Station. The GPR survey areas within the proposed location of the Civic Center Transit Station and Halekauwila Street are both situated within the HHCTCP project corridor. The remaining four survey areas have been previously investigated via subsurface testing and/or archaeological monitoring by Cultural Surveys Hawaii, Inc. (CSH) (Pfeffer et al. 1993, Pammer et al. 2009, Yucha et al. 2011). During these prior archaeological investigations, subsurface cultural deposits, including human burials, were identified within stratigraphic contexts that are similar to those that are anticipated to be present within the HHCTCP project corridor. Thus, the four survey areas located outside of the HHCTCP project corridor were investigated in an attempt to model how subsurface cultural deposits, including human burials, are mapped with GPR and then apply these models to GPR data collected within the HHCTCP project corridor. The results of these surveys would address

the efficacy of utilizing GPR to identify the presence of subsurface cultural deposits, including human burials, prior to subsurface testing.

Each area was collected with three different antenna frequencies: the 900 MHz antenna (the highest frequency antenna used), the 400 MHz antenna, and the 270 MHz antenna (the lowest frequency antenna used). The varying depth penetrations achieved with each antenna frequency at each location are summarized in Appendix A. In addition, a number of equipment calibrations and collection parameters for each antenna were performed at each site, and this technical information is summarized in Appendix B. All GPR data were collected between November 3 and 7, 2010 using a GSSI SIR-3000 control unit and survey wheels.

GPR Use and Background

Ground-penetrating radar data are acquired by transmitting pulses of radar energy into the ground from a surface antenna, reflecting the energy off buried objects, features, or bedding contacts and then detecting the reflected waves back at the ground surface with a receiving antenna. When collecting radar reflection data for archaeology or historic preservation, surface radar antennas are moved along the ground in transects, typically within a surveyed grid, and a large number of subsurface reflections are collected along each line. As radar energy moves through various materials, the velocity of the waves will change depending on the physical and chemical properties of the material through which they are traveling (Conyers 2004). The greater the contrast in electrical and magnetic properties between two materials at an interface, the stronger the reflected signal, and therefore the greater the amplitude of reflected waves (Conyers 2004). When travel times of energy pulses are measured, and their velocity through the ground is known, distance (or depth in the ground) can be accurately measured (Conyers and Lucius 1996). Each time a radar pulse traverses a material with a different composition or water saturation, the velocity will change and a portion of the radar energy will reflect back to the surface and be recorded. The remaining energy will continue to pass into the ground to be further reflected, until it finally dissipates with depth.

The depths to which radar energy can penetrate, and the amount of resolution that can be expected in the subsurface, are partially controlled by the frequency (and therefore the wavelength) of the radar energy transmitted (Conyers 2004). Standard GPR antennas propagate radar energy that varies in frequency from about 10 megahertz (MHz) to 1000 MHz. Low frequency antennas (10-120 MHz) generate long wavelength radar energy that can penetrate up to 50 m in certain conditions, but are capable of resolving only very large buried features. In contrast, the maximum depth of penetration of a 900 MHz antenna is about one meter or less in typical materials, but its generated reflections can resolve features with a maximum dimension of a few centimeters. A trade-off therefore exists between depth of penetration and subsurface resolution. In this survey, three different antenna frequencies were used: a 900 MHz antenna, a 400 MHz antenna, and a 270 MHz antenna. In general, the 270 MHz antenna achieved the greatest depth penetration, approximately 1 to 2 meters in most areas, while the 400 MHz antenna achieved the clearest resolution while also reaching the features of interest. The 900 MHz antenna, while providing outstanding resolution, could not penetrate deep enough to resolve most features of interest, reaching a maximum depth of about 50 centimeters in most

areas. With the 400 MHz and 270 MHz antennas, good data resolution was achieved at depths up to about 1.5 meters (just under five feet). Below this depth, energy attenuation occurred, likely due in large part to the water table, which is primarily saline (electrically conductive) water. In addition, extraneous noise sources from nearby power lines, radio frequencies, and other urban "noise" overwhelmed the very weak radar energy that had been attenuated at about 5 feet depth. Any features located below this depth could not be imaged.

The success of GPR surveys in archaeology, historic preservation, and cemetery studies is largely dependent on soil and sediment mineralogy, clay content, ground moisture, depth of burial, and surface topography and vegetation. Electrically conductive or highly magnetic materials will quickly attenuate radar energy and prevent its transmission to depth (Conyers 2004). The best conditions for energy propagation are therefore dry sediments and soil, especially those without an abundance of clay. The surveys in this project were all conducted on asphalt and concrete- paved surfaces, and the only surface obstructions included some parking medians in the Kaka'ako Fire Station parking lot. All of the antennas were therefore able to maintain good contact with the ground in these areas, and overall good energy propagation was achieved to depth.

The "time window" within which the GPR data were gathered ranged from 20 to 65 nanoseconds. This is the time during which the system is "listening" for returning reflections from within the ground. The greater the time window, the deeper the system can potentially record reflections, up to the point of attenuation. To convert time in nanoseconds to depth, it was necessary to determine the elapsed time that transpired for the radar energy to be transmitted, reflected, and recorded back at the surface by doing a velocity test. For this project, this was done using the program *FieldView*, in which hyperbolas found on reflection profiles are measured to yield a relative dielectric permittivity (RDP), which is a way to calculate velocity. The shape of hyperbolas generated in this program is a function of the speed at which energy moves in the ground, and can therefore be used to calculate velocity (Conyers 2004). In this project, each collection area had a slightly different RDP, indicating that energy is travelling through the ground at different speeds based on the sediment mineralogy and water content in each area, as discussed above. The calculated RDPs are discussed individually for each area below, but in general, all areas have an RDP which, when converted to one-way travel time (the time it takes the energy to reach a reflection source), ranges from approximately 3.5 to 5 centimeters/nanosecond (ns). For each of the grids, all profiles and processed maps were converted from time in nanoseconds to depth in meters using the average velocity for each area. These RDPs and calculated velocities are also summarized in Appendix A.

Data Processing Procedures

The initial data processing for this project involved the generation of amplitude slice-maps (Conyers 2004). Amplitude slice-maps are a three-dimensional tool for viewing differences in reflected amplitudes across a given surface at various depths. Reflected radar amplitudes are of interest because they measure the degree of physical and chemical differences in the buried materials. Strong, or high amplitude, reflections often indicate denser or different buried materials, such as archaeological features or burials. Amplitude slice-maps are generated through

the comparison of reflected amplitudes between the reflections recorded in vertical profiles. In this method, amplitude variations, recorded as digital values, are analyzed at each location in a grid of many profiles where there is a reflection recorded. The amplitudes of all traces are compared to the amplitudes of all nearby traces along each profile. This database can then be "sliced" horizontally and displayed to show the variation in reflection amplitudes at a sequence of depths. The result is a map that shows amplitudes in map view, but also with depth in the ground. Often when this is done, changes in the soil related to disturbances such as archaeological or burial features can become visible, making many features visible to the human eye that may not be visible in individual profiles. For this project, this was done using the program *GPR Process*.

From the original .dzt files (raw reflection data), a series of image files were created for cross-referencing to the amplitude slice-maps that were produced. Two-dimensional reflection profiles were also analyzed to determine the nature of the features identified on the amplitude slice-maps. The reflection profiles showed the geometry of the reflections, which can lead to insights into whether the radar energy is reflecting from a flat layer (seen as a distinct band on a profile), or a single object or burial (seen as a hyperbola in profile). Using these profiles to confirm or refute ideas about the nature of the buried materials seen in the three-dimensional slice maps, features of potential cultural interest were then delineated within the GPR survey areas.

Data Interpretation

Alapai Transit Center

One grid measuring four by seven meters was collected over two previously excavated trenches in the parking lot where the future Alapai Transit Center will be located (Figure 1). Two full burials and one partial burial were located by CSH within these trenches, and left *in situ* (Pammer et al. 2009). The GPR grid collected here was to test if and how these burials appeared in the amplitude slice-maps and reflection profiles.

The amplitude slice-maps generated for this grid were not effective for visualizing the spatial arrangement of the burial pits known to exist in this area. As shown in Figure 2, the majority of the high amplitude reflections (shown in red) relate to the previously excavated trenches by CSH, including the edges of these trenches and fill within these trenches. This is not surprising, given that the disturbed sediments from these trenches are likely much more reflective than the subtler reflections from the burial pits and other possible burials. Given that the high amplitude reflections in these maps did not form a recognizable pattern, identifying reflections relating to possible burials in this area therefore had to be accomplished through manual analysis of the GPR reflection profiles. This involved identifying all reflections of potential interest, and then plotting them to see how they related to the locations of the known burial pits and CSH trenches. When this was done, several reflections were found to relate to the edges of the known burial pits (Figure 2). This suggests that in these sediments, the stratigraphic disturbances generated from digging the burial shaft may be reflected better than the burial itself. Reflections that corresponded to locations within the trenches are likely buried objects within the trench fill. Other noted reflections that fall outside of the trenches may be related to additional possible burial pits, or other buried objects, such as historic debris or construction fill. Given the presence of other known burials in this small area, we would highly recommend treating all identified

reflections as potential burials, should further excavations occur in this area. Figure 3 below shows the reflections in a GPR reflection profile that correspond to the location of a known burial, as well as the reflection from a possible unmarked burial. Figure 4 also shows the reflection from a possible unmarked burial, as well as the clear stratigraphic breaks relating to the two CSH trenches. The locations of both these profiles are noted in Figure 1.

The RDP here was calculated at 17.1, which, when converted to one-way travel time, equals a velocity of approximately 3.6 cm/ns. Of the three antennas tested, the 400 MHz provided the clearest resolution of the features of interest (Figure 4). The maximum depth penetration achieved with this antenna is approximately 90 cm, and while the 270 MHz did propagate energy deeper (approximately 1.05 meters), it was not able to resolve target features, including the burials (Figure 5). The 900 MHz, on the other hand, provided superior resolution, but only within the upper 50 centimeters of the subsurface (Figure 6). As shown in the stratigraphic information in Figure 7, the majority of the target features occur within the first meter of subsurface, which is the depth achieved with the 400 MHz. The depths of the burial features noted in the GPR profiles are consistent with those recorded by CSH (Pammer et al. 2009) (Figure 7). Any burials that occur below this depth would be difficult to image in the GPR data.

Figure 1: GIS image showing the location of the GPR grid collected at the Alapai Transit Center. Also shown are the positions of the two trenches previously excavated by CSH. At the time of collection, these trenches had a wooden barrier surrounding them. The GPR grid was positioned to fit within this wooden barrier. Image courtesy of Jon Tulchin of CSH.

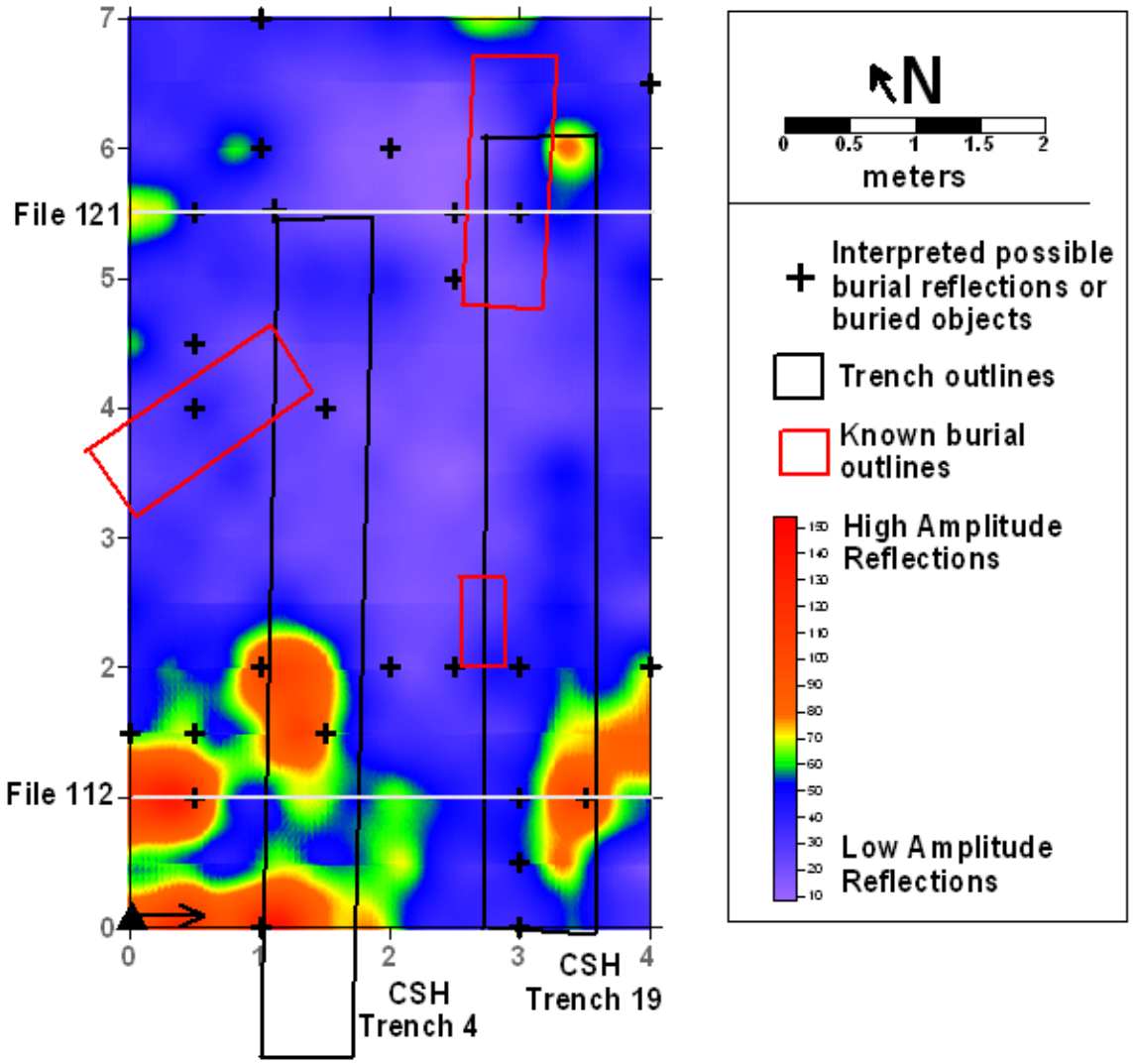

Figure 2: Amplitude slice-map with reflections of potential interest noted. Also shown are CSH trench locations and the known burial pit locations. As evidenced by this amplitude slice-map, which represents a depth of 16-20 ns, or approximately 60-75 cm, the majority of high amplitude reflections are generated from disturbance related to the previously excavated CSH trenches. Other areas of high amplitude reflections do not appear to form a recognizable pattern, and very few reflections are seen to correspond with the known burial pits. This is likely due to the subtler reflections related to these burial pits and other possible burials, which were identified in the reflection profiles and manually added to this slice-map. When this manual analysis was done, the correspondence of some of the noted reflections to the edges of the known burials suggests that GPR mapping is better able to resolve the shafts of burials or stratigraphic disturbance related to the burials, rather than the burials themselves. This slice-map was generated from data collected with the 400 MHz antenna

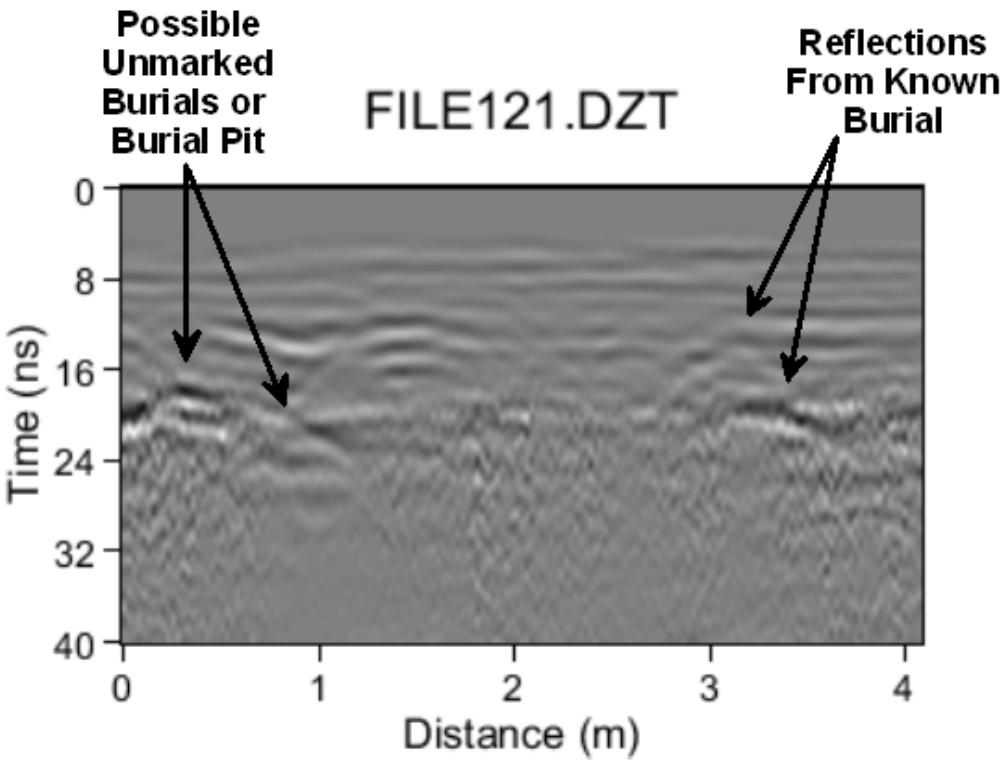

Figure 3. Reflection profile from the Alapai GPR grid showing the reflections from a known burial uncovered by CSH (recorded as Site 50-80-14-6902, burial pit burial 2). Also shown are the reflections from what may be an additional burial pit that occurs outside the trench boundaries. With a calculated velocity of approximately 3.6 cm/ns, this possible burial occurs at about 72 cm. This profile was collected with the 400 MHz antenna.

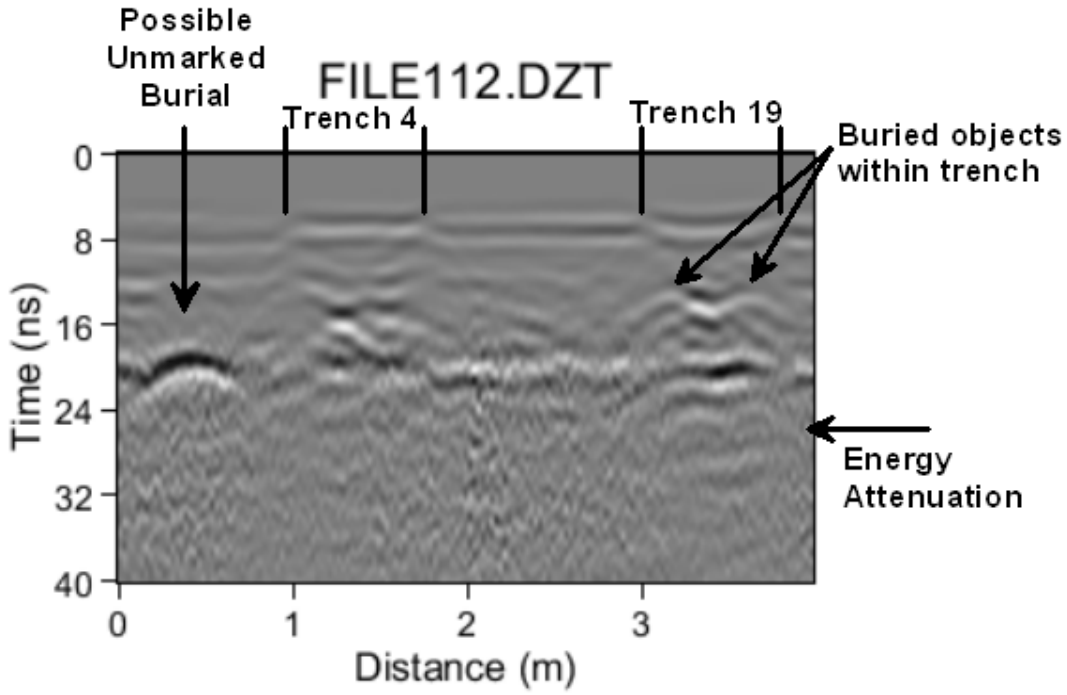

Figure 4: Reflection profile collected in a west-east direction with the 400 MHz antenna at Alapai. Even though energy attenuation occurs at approximately 25 ns (about 90 cm in depth), the resolution of the features of interest is the clearest of the three antennas tested here. Clearly seen are the stratigraphic breaks from the two trenches, as well as the hyperbolic reflection from what may be an unmarked burial. With a calculated velocity of approximately 3.6 cm/ns, this possible burial occurs at about 72 cm.

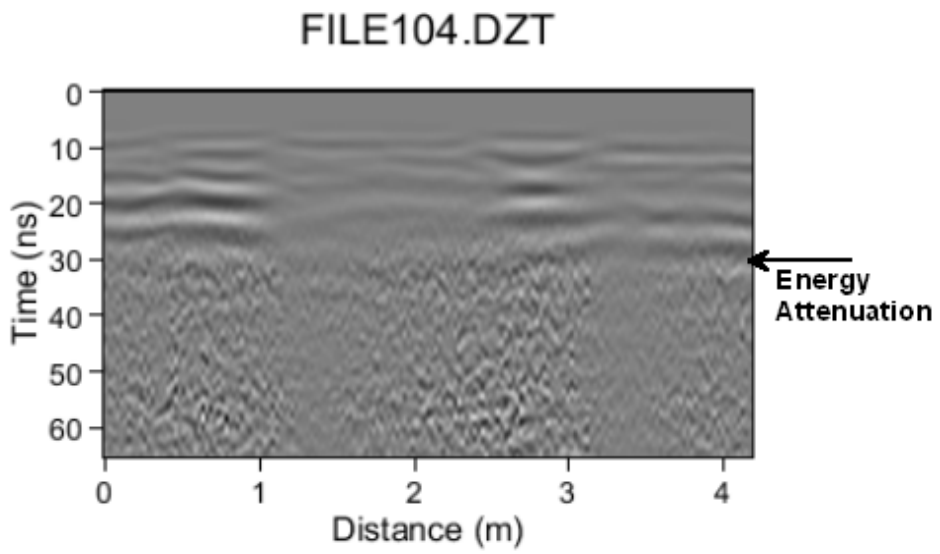

Figure 5: Reflection profiles collected with the 270 MHz antenna showing energy attenuation at approximately 30 ns, or just over one meter in depth. This antenna frequency was not effective for resolving burials in the Alapai area.

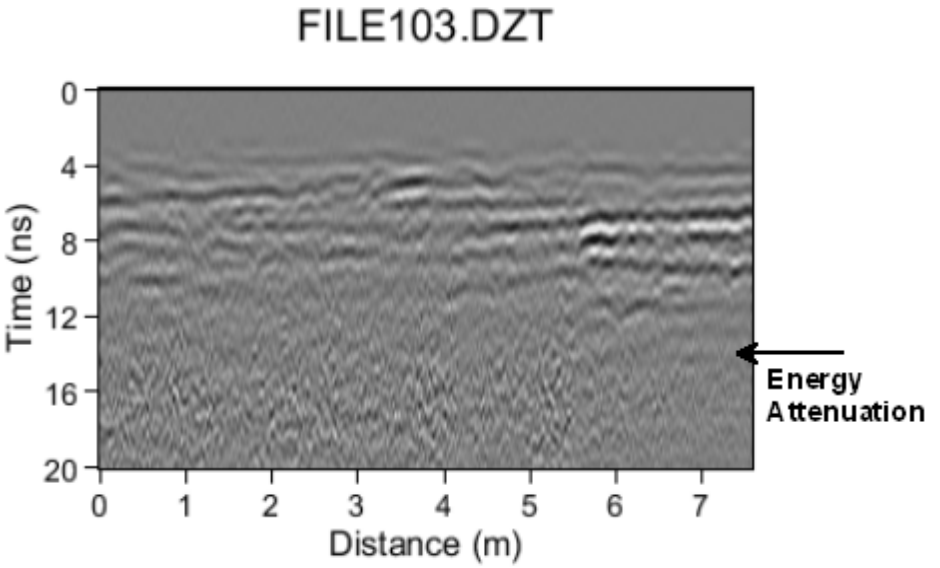

Figure 6: Reflection profiles collected at the Alapai grid with the 900 MHz antenna, showing energy attenuation at about 15 ns, or approximately half a meter in depth. Like the 270 MHz, this antenna frequency was not effective for resolving burials in this area.

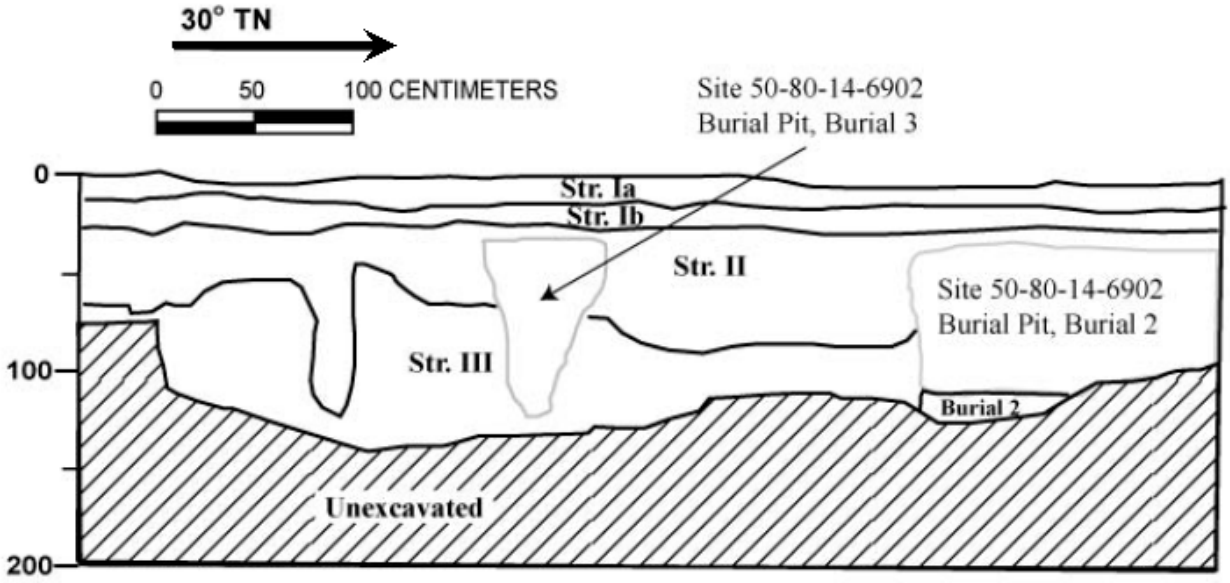

Figure 7: Stratigraphic information from Trench 19, North Wall Profile, with Burials 2 and 3 of Site 50-80-14-6902, excavated by CSH. A large part of the target features occur within the first meter of the subsurface, which was confirmed with GPR mapping with the 400 MHz antenna. Image courtesy of Matt McDermott of CSH.

St. Augstine Church

Six individual transects were collected with each antenna at St. Augustine Church (Figure 8) around the previously excavated trench (Figure 9). Transects were not collected over the trench itself due to the presence of a makeshift memorial. Even without collecting data directly over the trench, the GPR transects that were collected on the east side of the trench (T1 in Figure 9) showed reflections from a burial pit feature, which was confirmed by comparing the GPR transects to the trench profile drawing provided by CSH (Figure 10). Interestingly, the burial features recorded in the excavated trench were identifiable in the reflection profiles from all three antennas (Figure 11, Figure 12, Figure 13). This is likely due to the stratigraphic break characterizing burial pit #1, which occurs at a shallow depth and is distinct enough that it is reflected with all three frequencies.

Even given the very different spatial locations of St. Augustine and Alapai, the velocities were similar, suggesting that the radar energy is travelling through the subsurface materials in similar ways at both locations. The RDP at St. Augustine was calculated to be 16.4, which converts to approximately 3.7 cm/ns in one-way travel time. Also similar to Alapai, the maximum depth penetration achieved with any antenna was just over one meter (approximately 1.1 meters with the 270 MHz, one meter with the 400 MHz, and about half a meter with the 900 MHz). The main difference between the two locations was that the stratigraphic break characterizing the burial pit at St. Augustine could be identified with all three antenna frequencies, while at Alapai, only the 400 MHz antenna successfully resolved the burial features.

Figure 8: GIS image showing the location of the GPR survey area at the St. Augustine Church in Waikiki. Image courtesy of Jon Tulchin of CSH.

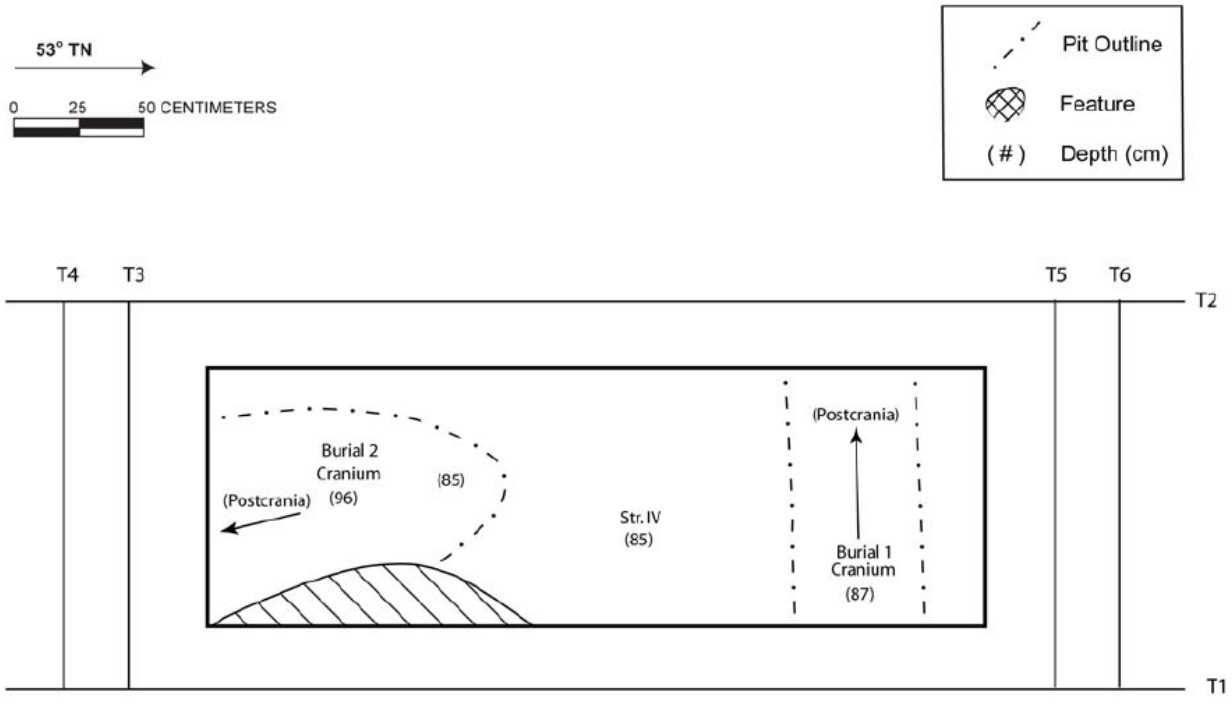

Figure 9: Plan-view drawing showing the positions of the burial features excavated within the trench by CSH, as well as the locations of the six GPR transects (labeled T1-T6) collected with each antenna frequency around the trench. Transects were not collected directly over the trench due to the presence of a makeshift memorial. Image courtesy of Jon Tulchin of CSH.

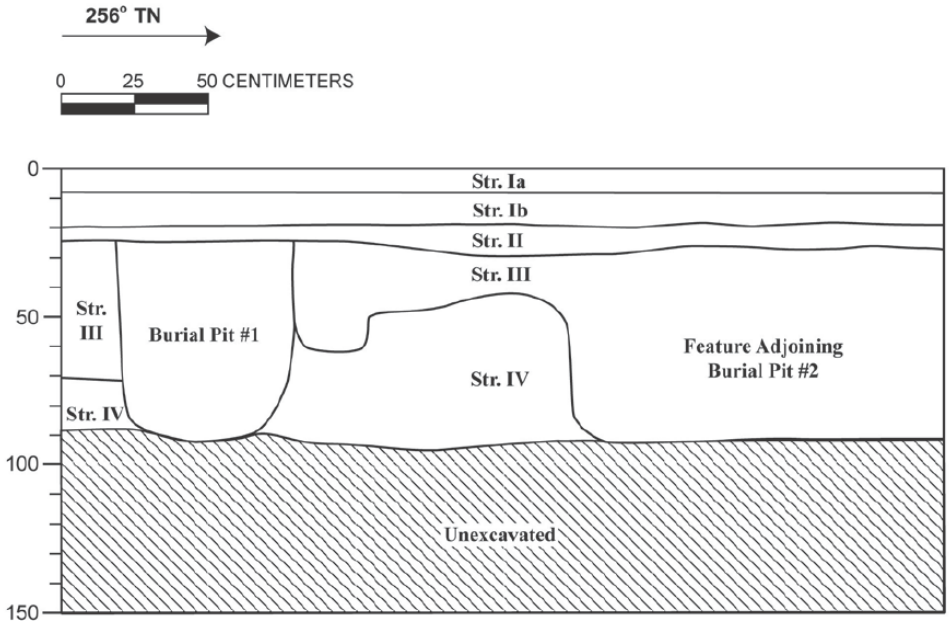

Figure 10: Profile drawing of the eastern wall of the trench in Figure, showing the locations of the burial features and stratigraphic layers. Image courtesy of Matt McDermott and Jon Tulchin of CSH.

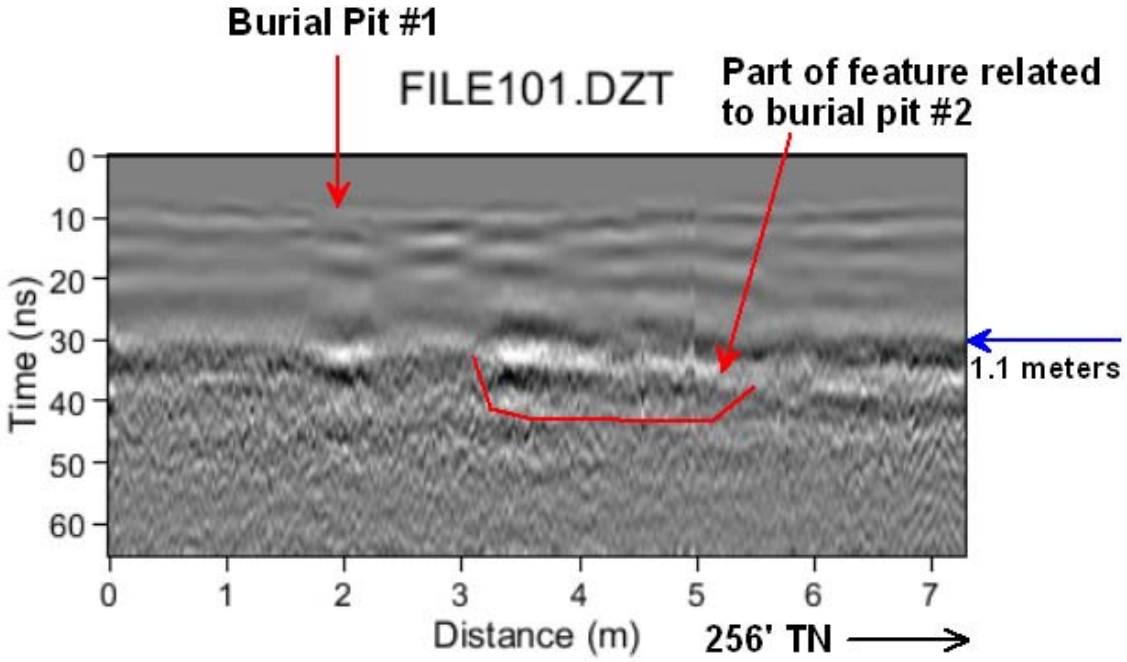

Figure 11: Reflection profile of transect 1 (T1), oriented in the same direction as the drawing in Figure. Collected directly next to the trench, this profile shows the reflections from burial pit #1, as well as from the feature associated with burial pit #2. Also noted is the level of energy attenuation, which occurs at 1.1 meters in depth. This profile was collected with the 270 MHz antenna.

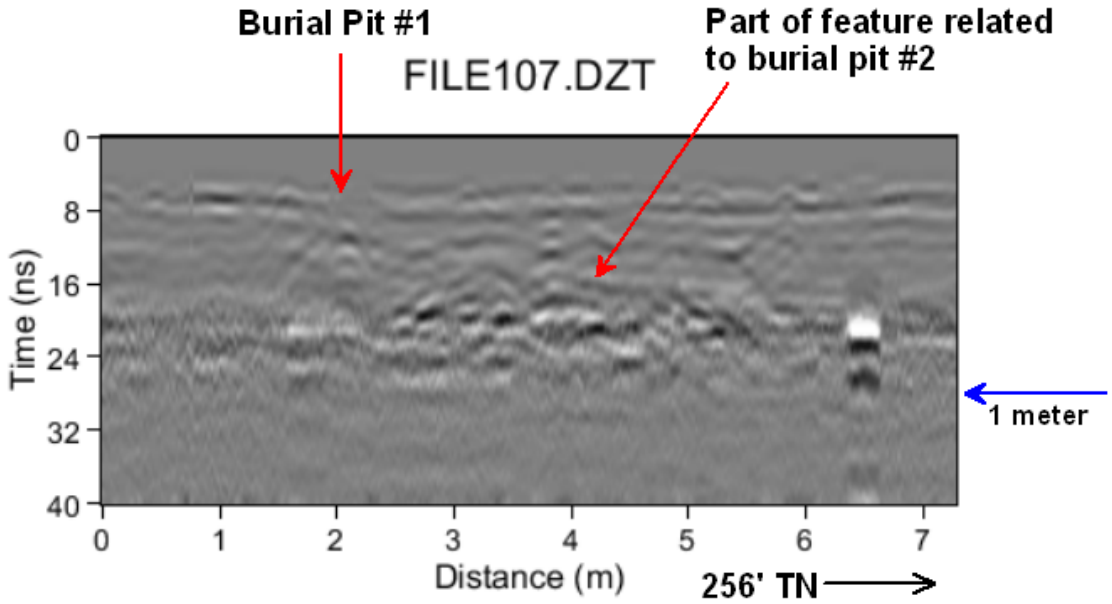

Figure 12: The 400 MHz antenna reflection profile of transect 1 (T1). The maximum depth of penetration with this antenna was approximately one meter. This profile shows a slightly higher resolution of both burial pit #1 and part of the feature associated with burial pit #2.

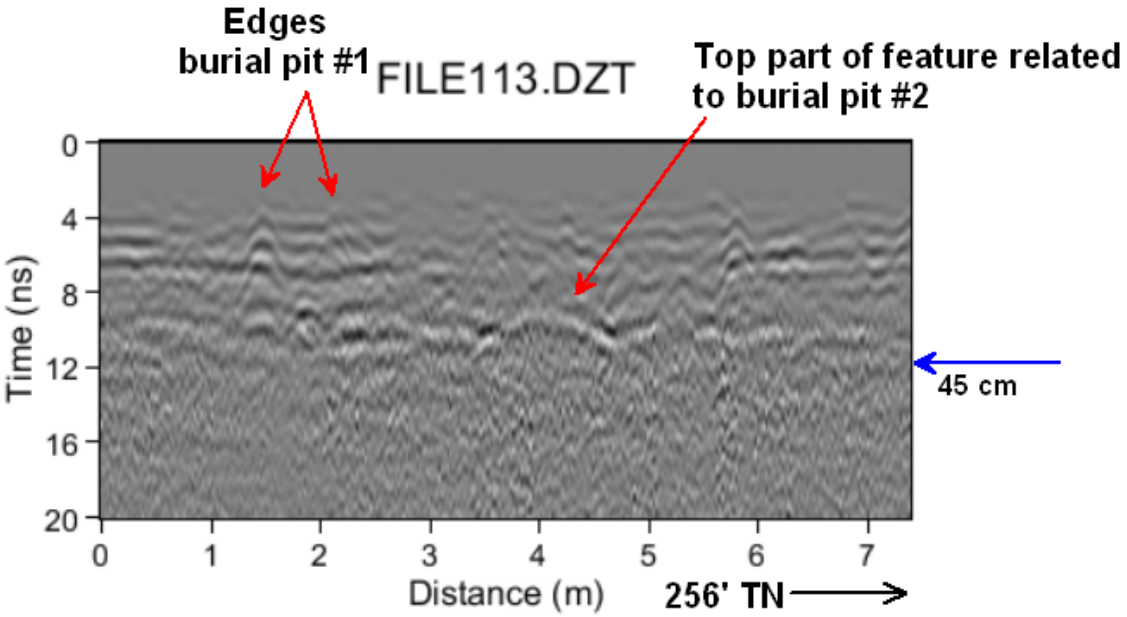

Figure 13: The same profile of transect 1 (T1), only collected with the 900 MHz antenna. While only reaching a maximum penetration depth of about half a meter, the edges of burial pit #1 and the top portion of burial pit #2 were imaged using this frequency.

Civic Center Transit Station

One grid area measuring 12 by 30 meters was collected with each antenna frequency in the parking lot where the Civic Center Transit Station will be located (Figure 14, Figure 15). A number of trenches have been previously excavated by CSH in this area, indicating a complex subsurface stratigraphy. In addition to assessing the overall resolution capabilities and depth penetration of each antenna, identifying how these stratigraphic layers were impacting the transmission and reflection of the radar energy was one of the main goals of the survey in this parking lot area.

The calculated RDP of this area is 18.5, which converts to a velocity of approximately 3.5 cm/ns. This RDP is very typical of saturated sand or sandy clay (Conyers 2004). The maximum depth penetration achieved here was just under approximately 1.5 meters with the 270 MHz antenna. Interestingly, the 400 MHz antenna was able to penetrate to a similar depth, nearly 1.2 meters, while the 900 MHz antenna's penetration depth was less than half a meter.

The maximum depth of 1.5 meters is not surprising given the known stratigraphy of this area, which, in addition to containing sandy clay, includes a hardened coral shelf at approximately this same depth of 1.5 meters (Figure 16). It is likely that the mineralogy of this coral layer (likely electrically conductive) is attenuating the GPR energy, preventing even the lowest frequency antenna from reaching beyond this depth.

Given the mineralogical constraint of this area's subsurface, which is limiting the overall penetration to about 1.5 meters regardless of the antenna frequency being used, a more important consideration is the level of resolution achieved within this 1.5 meter depth. While the 270 MHz is transmitting to the greatest depth of the three antennas, resolution of buried features is far inferior to the 400 MHz antenna. Figure 17, Figure 18, and Figure 19 below show a profile collected from each of the three antennas, each representing the same transect within the grid. While it is clear from all three profiles that there are reflections of note, the overall resolution of these reflections is superior in the 400 MHz profile. As seen in Figure 20, there are multiple hyperbolas in a concentrated area, indicating a number of "point sources" (individual objects that each generate a hyperbolic reflection) that are clustered together. These reflections may originate from historic debris or construction fill. This type of detailed analysis of these reflections is not possible with the 900 MHz profile (Figure 17) or the 270 MHz profile (Figure 19). Not only does this suggest that analyzing the reflection profiles is an important way to interpret the subsurface, but also that in this area, the 400 MHz antenna provides the best overall resolution of the subsurface while also reaching the target depth.

It should be noted that the buried objects marked in Figure 17, Figure 18, and Figure 19 are all seen clearly on the amplitude slice-maps created from each dataset (Figure 20). These buried objects are represented in Figure 20 by areas of red, indicating areas of higher density or highly reflective buried features. These slice-maps are important tools for visualizing the spatial extent of these objects, helping to determine, for example, that they are not related to utility pipes, as there is no linearity to them. Beyond an area of high reflections, however, there is little else to indicate what they might relate to, and this is true for all three of the antenna frequency datasets. As seen in Figure 20, the differences in the display of these reflections are not substantial enough between the 900 MHz, 400 MHz, and 270 MHz slice-maps to lend clarity as to the nature of

these reflections. When these slice-maps are analyzed in combination with the reflection profiles, however, it becomes possible to develop hypotheses about what these reflections may relate to based on their overall strength and geometry. So while each antenna frequency is able to map possible buried features in this area, as evidenced by the slice-maps, the reflection profiles collected with the 400 MHz antenna provide the optimal trade-off between resolution and depth penetration for identifying and analyzing the nature of these reflections.

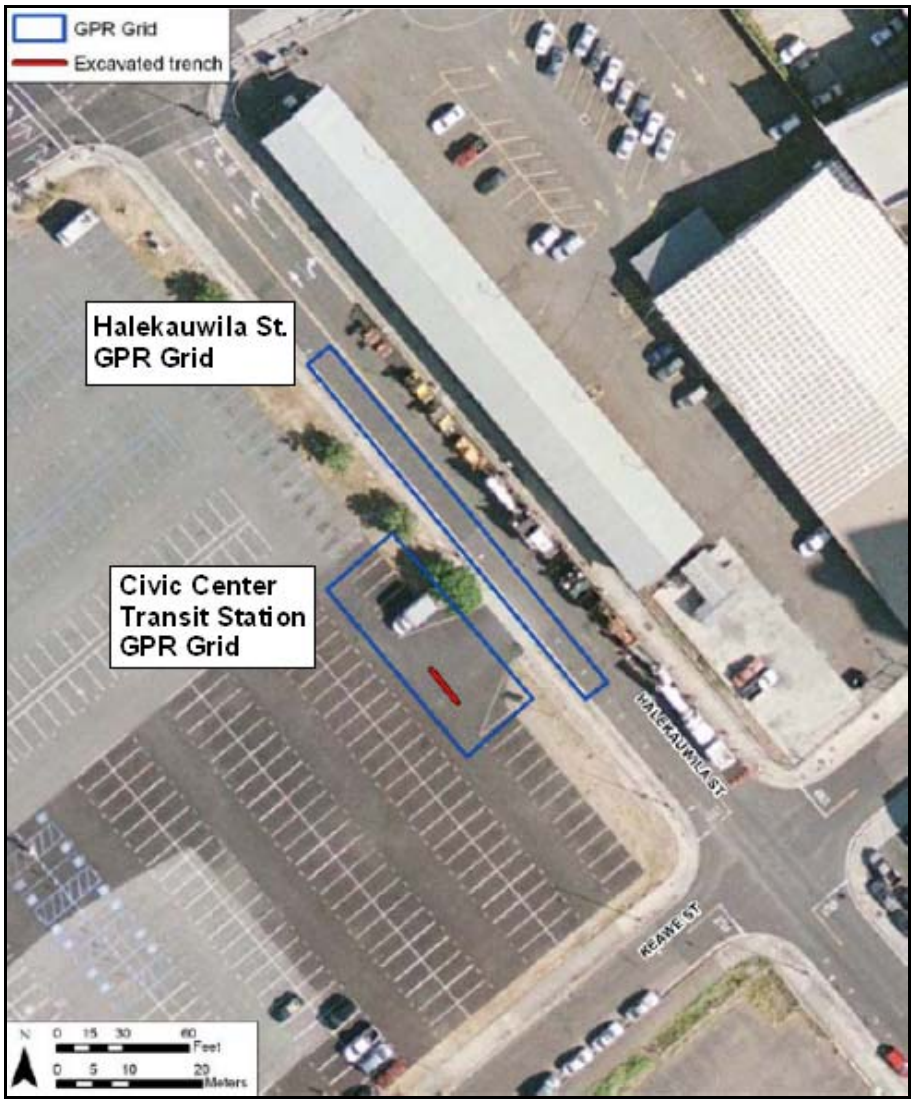

Figure 14: GIS image showing the locations of the GPR grid collected in the parking lot where the future Civic Center Transit Station will be located, and the GPR grid collected in Halekauwila Street. Image courtesy of Jon Tulchin of CSH.

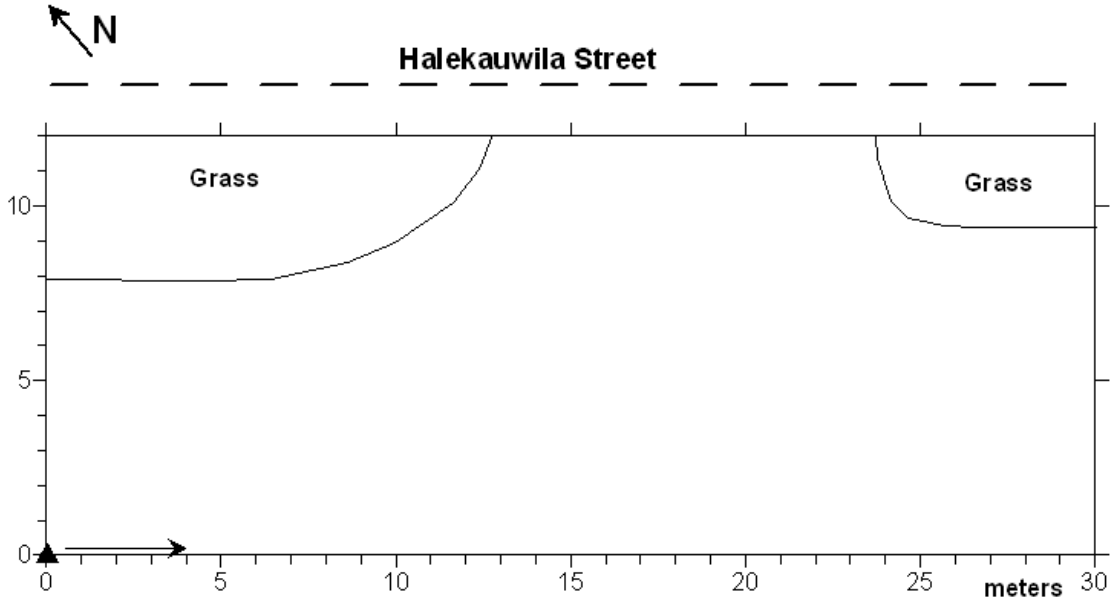

Figure 15: Sketch map of the Civic Center GPR grid, indicating the grassy areas and surveying direction.

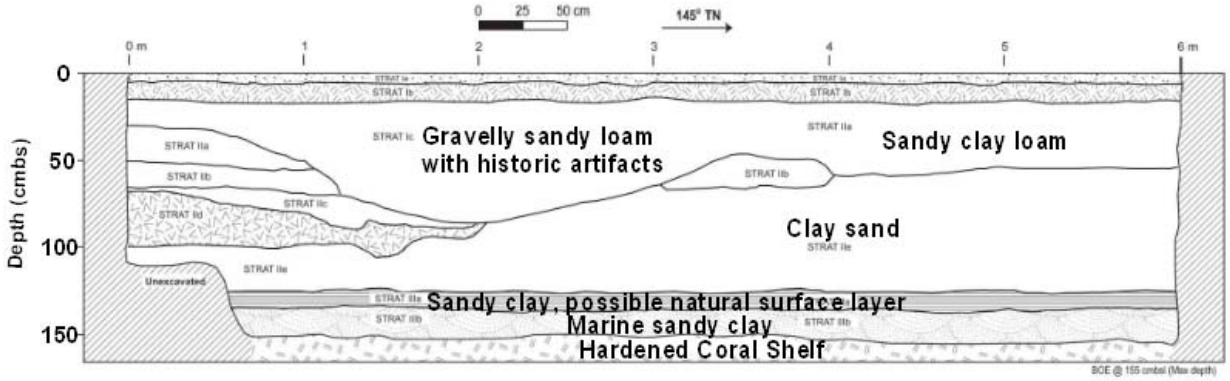

Figure 16: Profile drawing of one of the trench walls excavated in this parking lot by CSH. The main stratigraphic layers are labeled with information provided by CSH. Original image courtesy of Matt McDermott of CSH.

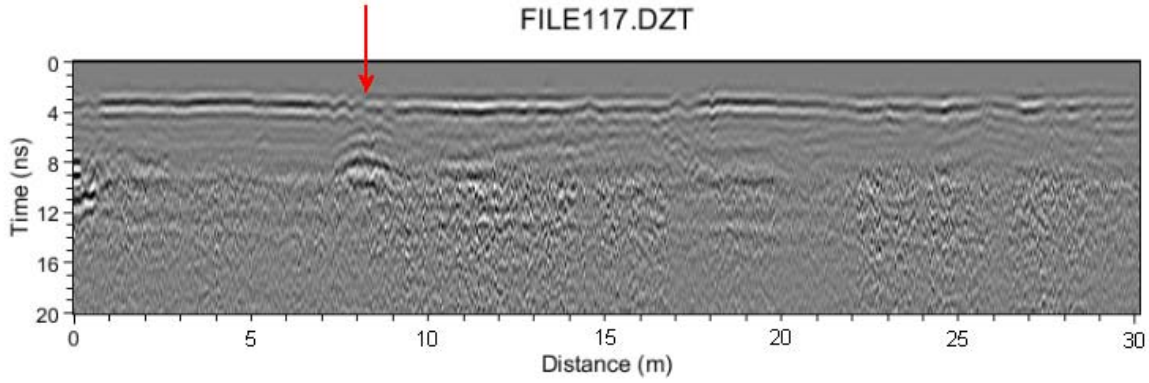

Figure 17: GPR reflection profile from the Civic Center grid, with an arrow indicating reflections from a buried feature or object. This profile was collected with the 900 MHz antenna, which had maximum depth penetration of about 45 cm.

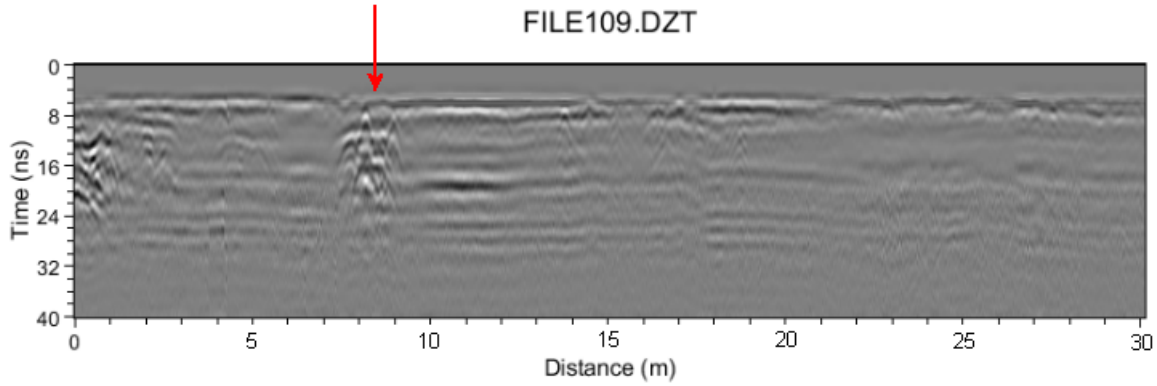

Figure 18: The same GPR profile as in Figure, but collected using the 400 MHz antenna. The arrow indicates reflections from the same buried objects. Because this antenna was able to propagate energy further, more of the buried objects are resolved. The maximum depth penetration with this antenna was approximately 1.2 meters.

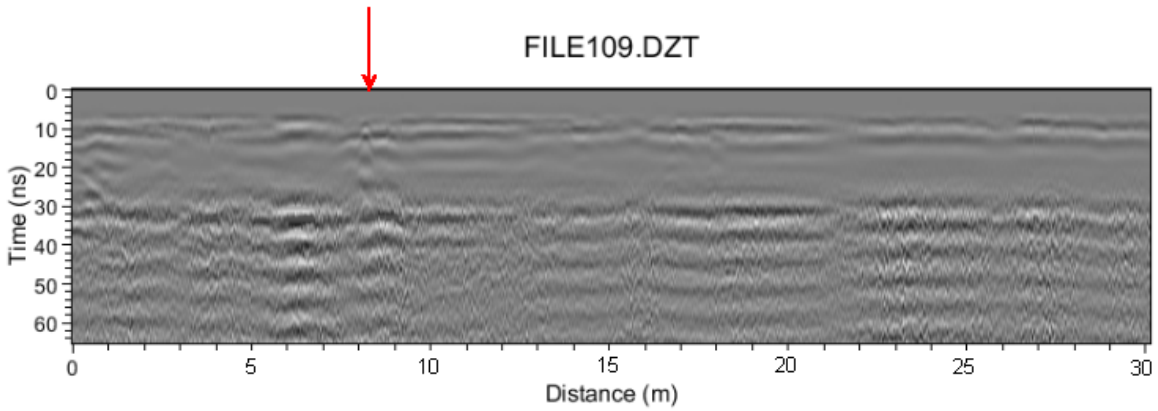

Figure 19: The same GPR profile shown in Figure and Figure, but collected using the 270 MHz antenna. The arrow indicates the same buried objects seen in the other profiles, though because of the longer wavelength of this antenna, less of the objects are resolved. The maximum depth penetration achieved with the 270 was about 1.5 meters.

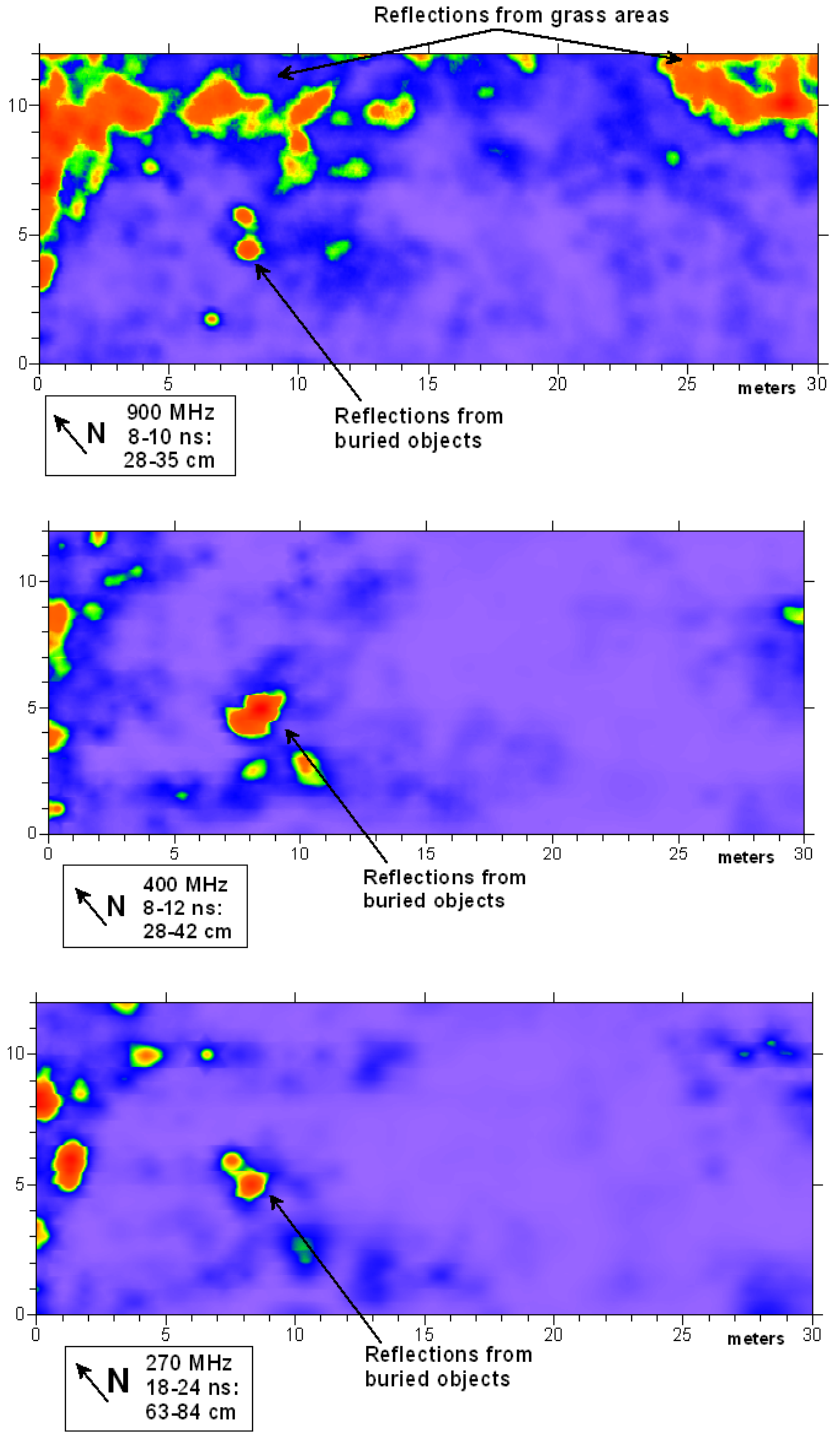

Figure 20: Amplitude slice-maps from the Civic Center Transit Station parking lot. The top map was generated from the 900 MHz dataset, the center map from the 400 MHz dataset, and the bottom map from the 270 MHz dataset. All three maps show the high-amplitude reflections (indicated by the red areas) from the buried objects shown in the reflection profiles in Figure, Figure, and Figure above.

Halekauwila Street

Two contiguous grids, each 3.5 by 30 meters, for a total of 3.5 by 60 meters, were collected in Halekauwila Street to test the GPR method in a road area with known utilities (Figure 14 and Figure 21). The maximum depth penetration achieved here was approximately 1.65 meters with the 270 MHz antenna, and within this depth, both the 270 MHz and 400 MHz antennas were very successful at mapping utility lines. Utilities or pipes that occurred below the depth of 1.65 meters could not be imaged due to energy attenuation. The 900 MHz antenna, which propagated energy to a depth of approximately 55 cm, was not able to resolve most of the utility lines.

Figure 22 below shows a series of amplitude slice-maps generated from the 400 MHz data, starting with the shallowest slice at the top and progressing deeper into the ground. As evidenced by these slice-maps, sections of the known utility pipes are apparent in certain slices, suggesting these utilities exist at various depths in the ground. In addition, the utilities that exist perpendicular to the GPR transect direction were mapped more clearly than those that run parallel to the GPR transects (the longer utility lines, as seen in Figure 21). This is because utilities that exist perpendicular to the GPR transects act as “point sources,” or single objects in the ground that generate a distinct hyperbolic reflection (Figure 23). Utilities in this area were identified both with the reflection profiles, which showed these characteristic hyperbolas, and with the slice-maps, which showed that these reflections map out in a linear way. Comparing these slice-maps with the map of known utilities, such as in Figure 21, further supports these interpretations.

Compared to the nearby Civic Center parking lot, the velocity in Halekauwila Street was slightly faster, with an RDP of approximately 10.5, or about 4.5 cm/ns. This variation may be due to differences in fill material between the street and parking lot. As described above, the resolution capabilities between the three antennas varied greatly. Figure 23 below shows the same transect collected with each different antenna (noted on Figure 22), and the differing resolution capabilities of the utilities here.

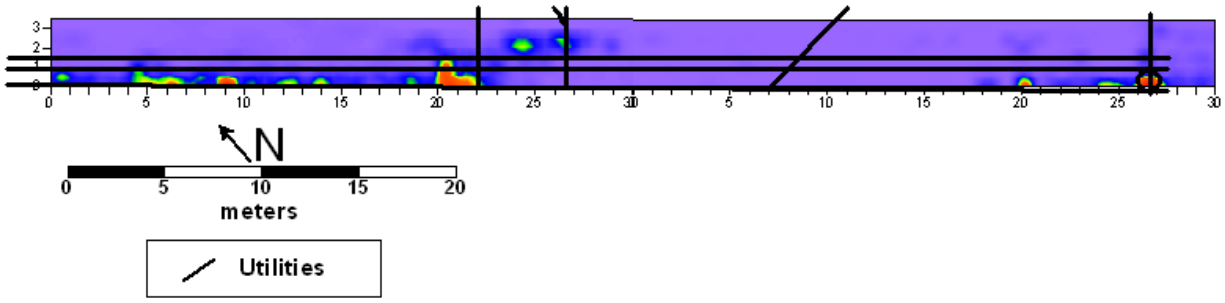

Figure 21: Amplitude slice-map of the two contiguous GPR grids collected in Halekauwila Street, with a map of the utilities overlain. Both the 400 MHz and 270 MHz antennas were able to map utilities that occurred within approximately 1.65 meters. This slice-map was generated from the 400 MHz data, and represents a depth of 20-24 ns, or approximately 90-108 cm.

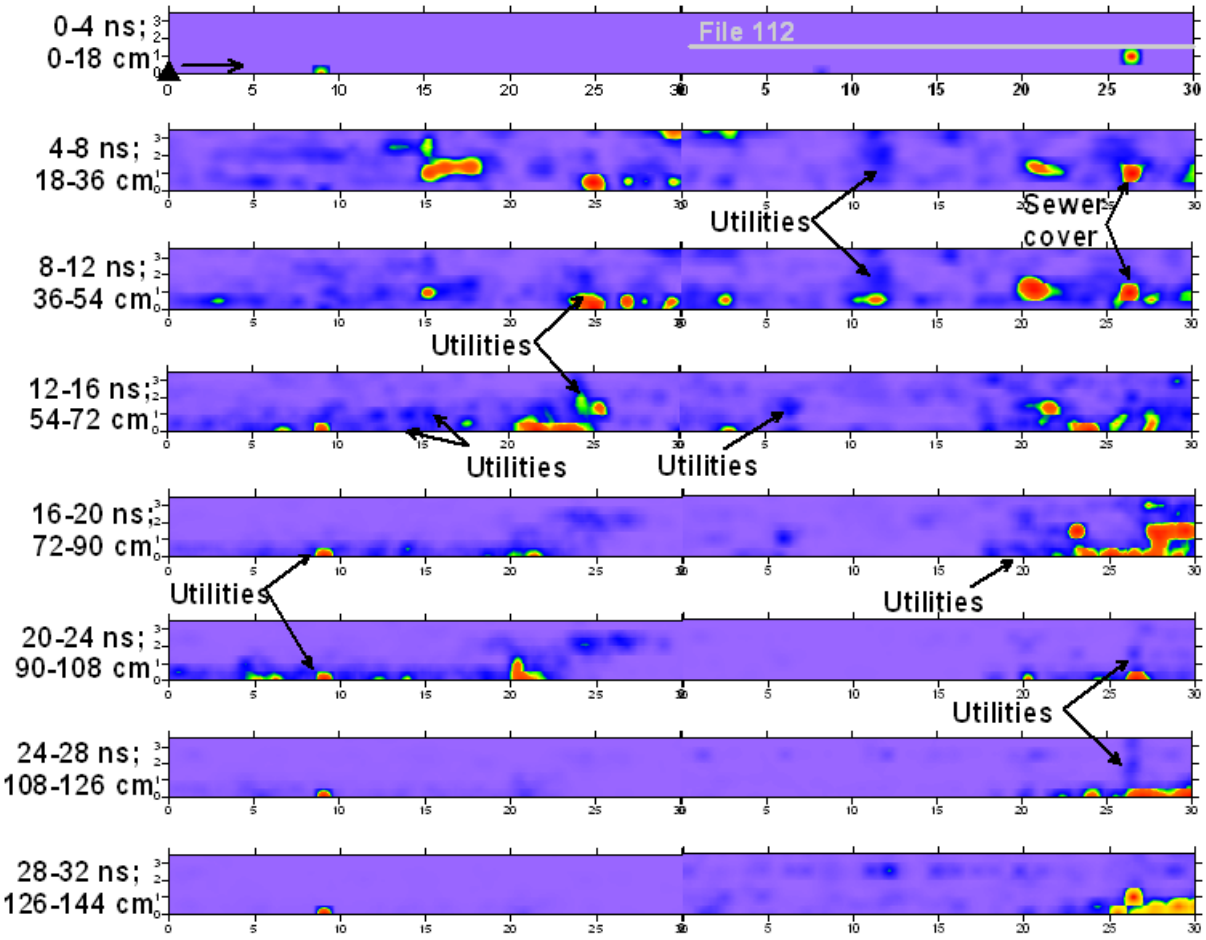

Figure 22: Series of amplitude slice-maps generated from the 400 MHz data collected in Halekauwila Street. Sections of the known utility pipes are seen in different slice-maps, suggesting these utilities exist at different depths. Also noted in the top (shallowest) map are the GPR surveying direction and the location of reflection profile 112 (file 112), which was collected with each of the three antenna frequencies and shown below in Figure 23.

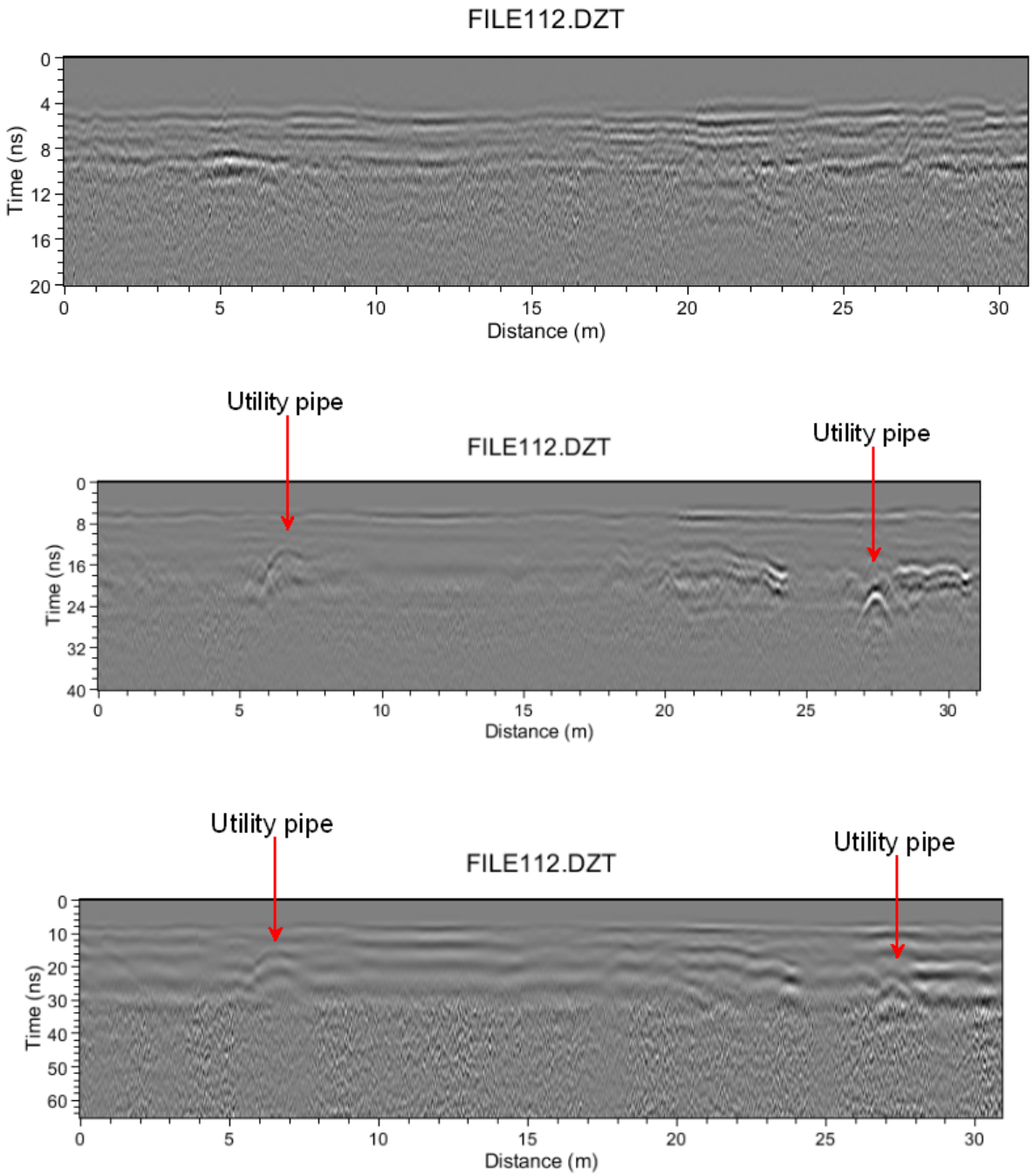

Figure 23: Reflection profiles collected in Halekauwila Street. All three profiles represent the same transect collected within one of the grids at Halekauwila Street, just collected with different antenna frequencies. The top profile was collected with the 900 MHz antenna, the middle profile with the 400 MHz antenna, and the bottom profile with the 270 MHz antenna. While the 900 MHz did not resolve any of the utility pipes, both the 400 MHz and 270 MHz were highly successful at mapping utilities that occurred within a depth of about 1.65 meters. The calculated velocity for this street is 4.5 cm/ns.

Kaka‘ako Fire Station

Back parking Lot/Asphalt Area/Smallpox Cemetery Area

Two GPR grids were collected at the Kaka’ako Fire Station (Figure 24 and Figure 25). The back parking lot/smallpox cemetery area had the most complex subsurface of any of the areas mapped with GPR. In addition to possible burials, several other features were mapped, including possible utility lines, fill material, and wire meshing within this fill. As with other areas, these features were, for the most part, mapped with all three antenna frequencies, though with varying degrees of resolution and depth penetration.

The calculated RDP for this area is approximately 12, which converts to a velocity of about 4 cm/ns. Compared to other areas, the overall greatest depth penetration and resolution was achieved here with all three antennas. The maximum depth penetration here was just over approximately 2.25 meters with the 270 MHz antenna, though the resolution was not great below about 1.75 meters (Figure 26). The 400 MHz antenna reached a depth of approximately 1.75 meters, with very good resolution within the entire time window (Figure 27). The 900 MHz antenna provided excellent data resolution up to about 16ns, or approximately 70 cm (Figure 28).

Figure 26, Figure 27, and Figure 28 below show four amplitude slice-maps generated from each of the antenna frequency datasets, as well as a reflection profile collected with each antenna, and each representing the same transect collected within the grid. As seen in the 270 MHz maps (Figure 26), larger, more deeply buried features are more readily resolved than with the 400 or 900 MHz antennas. This includes three possible utility lines, which were beyond the depth penetration of the 400 MHz. In addition, several buried objects were noted in the 270 MHz profiles, including what may be possible burials. Note, however, the differences in resolutions between the 270 MHz profile (seen in Figure 26) and 400 MHz profile (seen in Figure 27). Even though these profiles represent the same transect within the grid, the objects and burials in the 400 MHz profile are substantially clearer. What are seen as minimal reflections in the 270 MHz profile are clearly defined hyperbolic reflections in the 400 MHz profile. It was with the 400 MHz profiles, in fact, that the possible burials here were identified at all. So while the 400 MHz did not reach the same depth as the 270 MHz, and was thus not able to resolve certain features such as the possible utility lines, it was highly successful at resolving smaller features that occurred at shallower depths. If the majority of burials occur within the first two meters of the subsurface, then the 400 MHz antenna will be a better choice for mapping and resolving these features.

Also seen in the 400 MHz profile are the reflections from wire meshing that occur within the northwestern section of this parking lot (Figure 27). This wire meshing is also seen quite clearly in the 900 MHz profile, as well as the reflections from other fill material (Figure 28). While perhaps not a target feature of interest, understanding the overall subsurface stratigraphy here, including the presence of wire meshing, could be highly beneficial for future excavation planning.

In addition to the wire meshing, the reflections from the possible burials seen in the 400 MHz and 270 MHz profiles are also seen in the 900 MHz profile (Figure 28). Unlike the 400 MHz

profile, however, only the very uppermost portions of these features are resolved with the 900 MHz antenna. By about 70 cm in depth, most of the energy from this antenna has been attenuated, and very little is imaged below this depth.

While the reflection profiles are perhaps the most important images for assessing overall depth penetration and feature resolution in this area because they show the depth of energy attenuation as well as the vertical structure and geometry for buried features of interest, the amplitude slice-maps should not be discounted. What is evident from the generation of these slice-maps from each dataset is each antenna frequency is mapping and resolving different sections of the subsurface. For example, the slice-maps generated from the 270 MHz data show the deeply buried possible utility lines, while mapping very little of the fill material known to exist in the northwest section of this grid. The slice-maps generated from the 400 MHz data, on the other hand, clearly shows the high amplitude reflections from this fill material, as well as the reflections from other smaller objects that occur within the uppermost meter of the subsurface. Finally, the slice-maps generated from the 900 MHz data show the clearest resolution of this fill material, helping to spatially define individual objects that occur at the shallowest depths. While these are not necessarily of cultural interest in this area, the resolution capabilities of this antenna may have applications in other areas where smaller, shallower features need to be imaged.

It is important to emphasize that identifying and interpreting features of potential interest using GPR mapping depends greatly upon the specific site conditions and subsurface properties of the area to be surveyed. Certainly some generalizations can be made for analyzing GPR data (identifying “point source” hyperbolic reflections is a good example) and comparisons can be made using these analyses, such as using the burial reflections in one area to identify burial reflections in another nearby area. The most important considerations when identifying and interpreting any feature, however, are understanding the historic context of the area to be surveyed, and recognizing patterns in the geophysical datasets. For example, hyperbolic reflections found in areas where burials are known or hypothesized to exist are more likely to be interpreted as relating to other unmarked burials. In addition, interpreting possible burials must include pattern recognition. Hyperbolic reflections that occur in multiple consecutive profiles (thus forming a linear pattern) are likely related to buried utility pipes or walls, whereas a reflection from a burial (whether from a coffin or burial shaft) often occurs in only a couple consecutive profiles (depending on transect spacing). When these two considerations, historic context and pattern recognition, are utilized in a GPR survey, then GPR mapping is a valuable method for assessing the subsurface of an area, helping to remove some of the doubt of what will be impacted during excavation or construction. Without this type of non-invasive surveying, affected areas must be assumed to have features of interest, particularly in areas with known historic significance or where burials are hypothesized to exist.

Figure 24: GIS image showing the locations of the two GPR grids collected at the Kaka’ako Fire Station. One larger grid was collected in the back parking lot area, over part of what was once a smallpox cemetery. The second smaller GPR grid was collected in front of the fire station to compare the data resolution on concrete to asphalt. Image courtesy of Jon Tulchin of CSH.

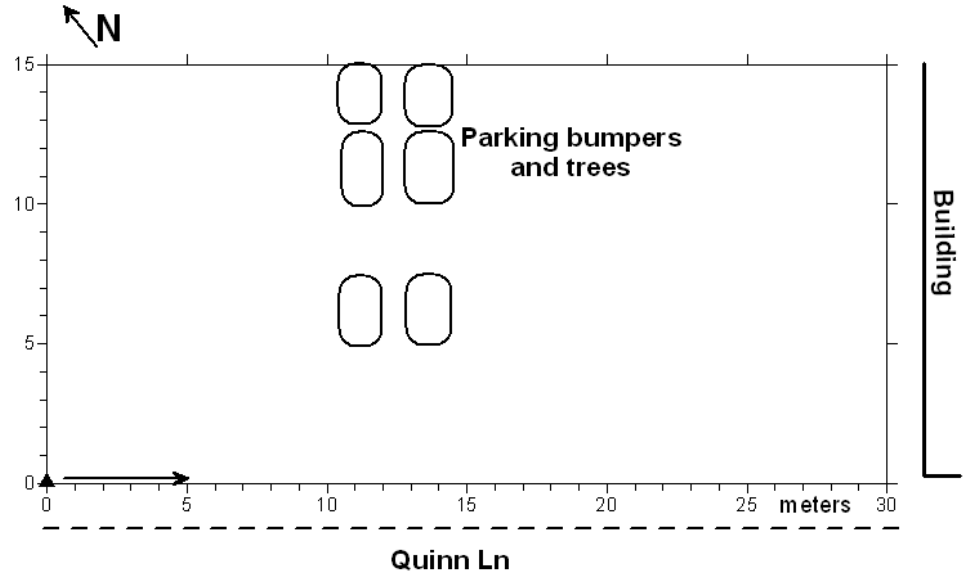

Figure 25: Sketch map of the GPR grid collected in the back parking lot/smallpox cemetery area at the Kaka’ako Fire Station. The locations of the parking bumpers and surveying direction are noted.

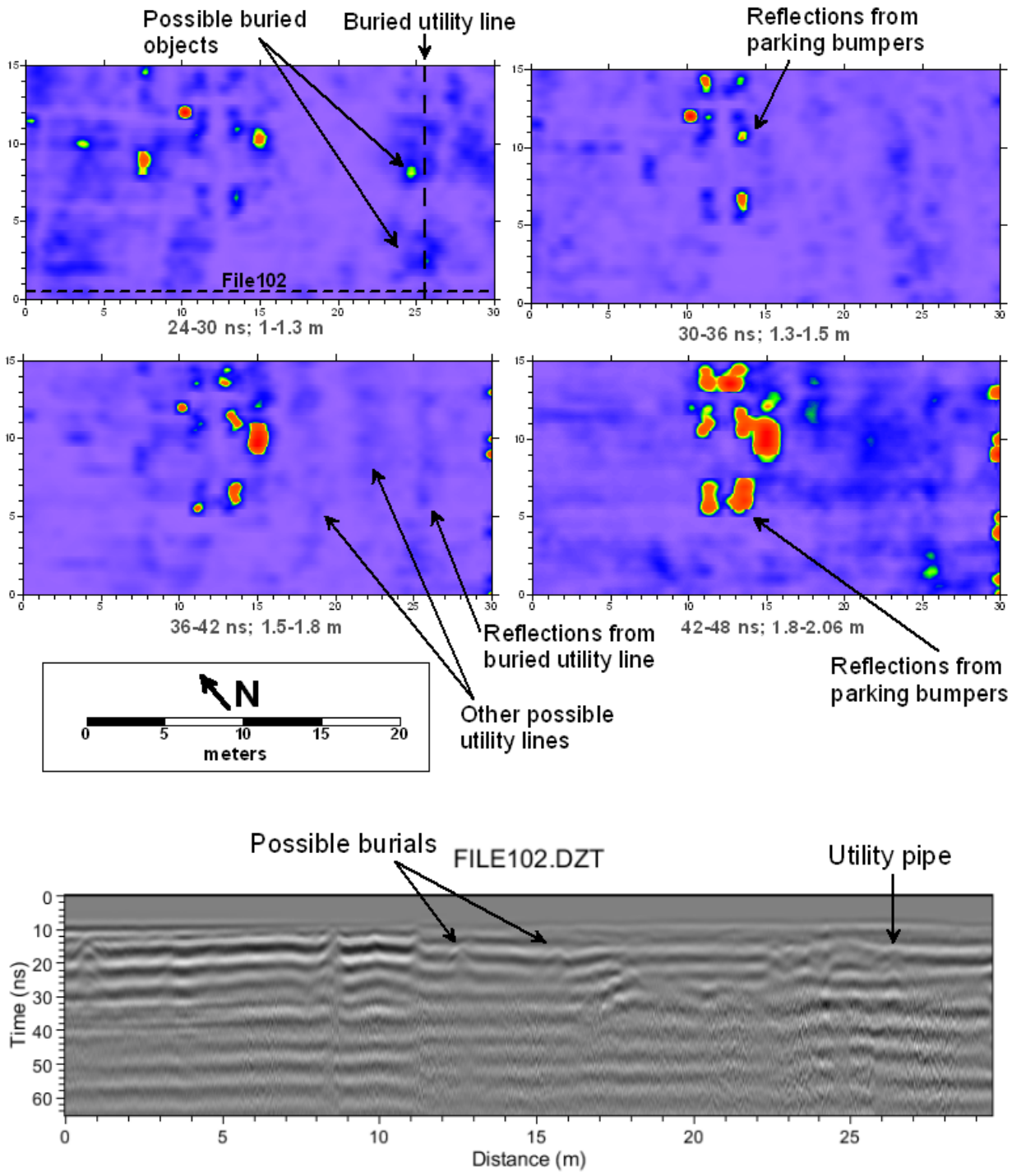

Figure 26: Amplitude slice-maps and reflection profile from the 270 MHz data collected in the parking lot at the Fire Station. The greater depth penetration of this antenna allowed three possible utility lines to be imaged here, as well as what may be burials or other objects. The calculated velocity here is 4 cm/ns, translating to an overall depth penetration with this antenna of approximately 2.25 meters.

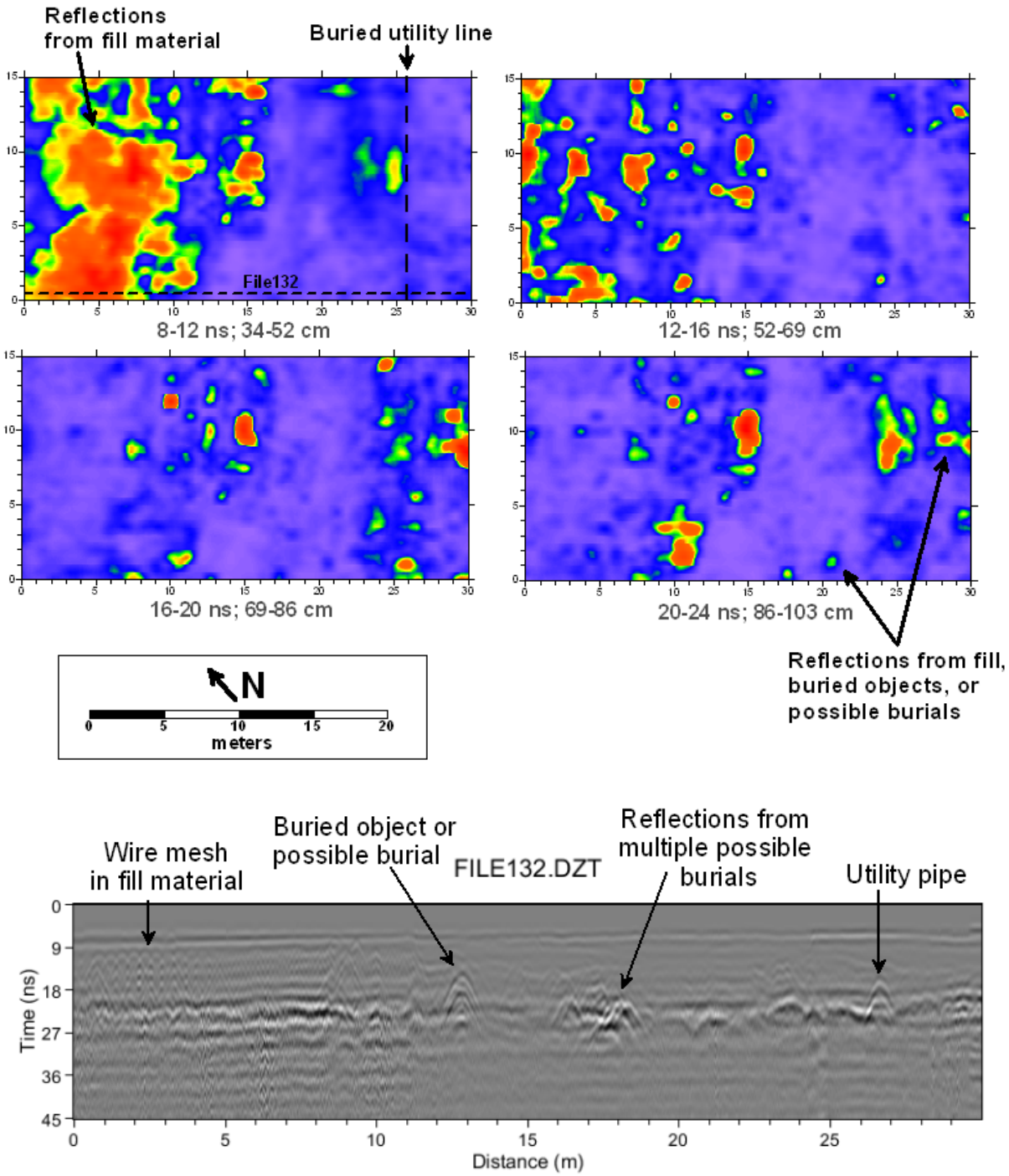

Figure 27: Amplitude slice-maps and reflection profile from the 400 MHz antenna data. The possible objects and burials seen in the 270 MHz profiles are clearly resolved here, showing a clearer overall geometry and shape. Also shown are the reflections from the fill material and wire meshing that exists in the northwestern section of this parking lot. The overall depth penetration achieved with this antenna was about 1.75 meters.

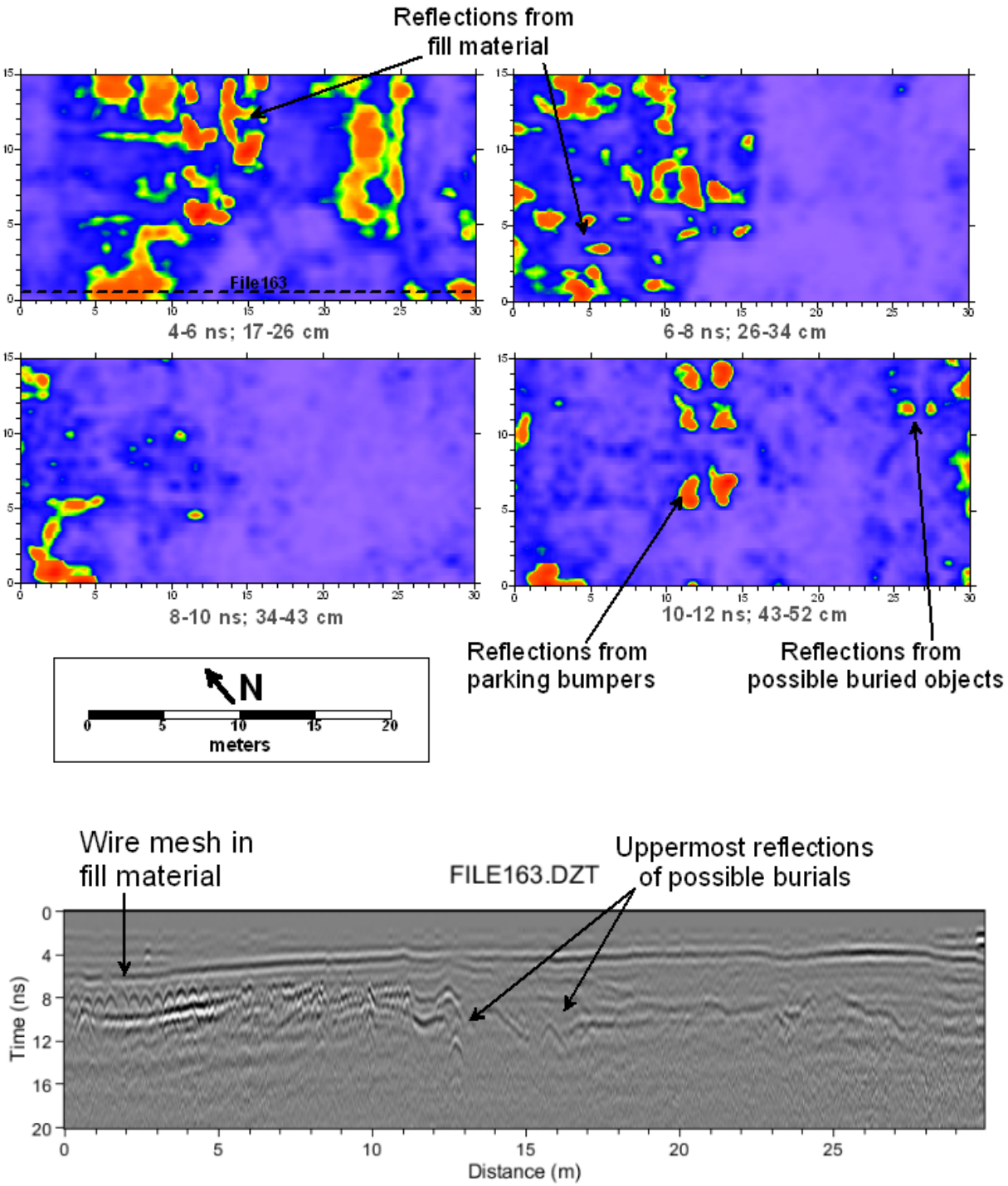

Figure 28: Amplitude slice-maps and reflection profile from the 900 MHz antenna data. This antenna provided excellent resolution of the wire meshing and fill material in this area, though only the uppermost portions of the possible burials are resolved. The overall depth penetration achieved with this antenna was about 70 cm.

Front Concrete Area

One grid measuring 8 by 12 meters was collected in the front area of the Fire Station specifically to test GPR mapping on concrete (Figure 24 and Figure 29). While no features of archaeological interest were noted in these datasets, this survey area provided a way to compare the overall resolution and depth penetration of the GPR data on concrete versus asphalt. One of the most obvious features within this concrete material is the presence of shallow wire mesh, which shows up well in the reflection profiles from all three antennas, though with varying resolutions (Figure 30, Figure 31, Figure 32).

The calculated RDP for this area is 9, which converts to a velocity of approximately 5 cm/ns. Not surprisingly, the 900 MHz antenna provided the highest resolution of the wire mesh, while the 270 MHz only resolved parts of the wire mesh, likely the larger sections of rebar that may exist within the wire meshing. Even with the presence of wire meshing, the 270 MHz still achieved a depth of approximately two meters, while the overall depth of the 900 MHz was about half a meter, which has been relatively consistent with other areas tested for this study. The 400 MHz antenna provided the most optimal trade-off for this area, achieving a maximum depth of approximately 1.3 meters with good resolution of the wire meshing. In addition to mapping this meshing, the 400 MHz antenna was able to resolve other possible features beneath the wire meshing. Figure 31 shows the reflection from what may be a utility line beneath the meshing, which is not seen in the corresponding transects from either the 900 MHz or 270 MHz datasets.

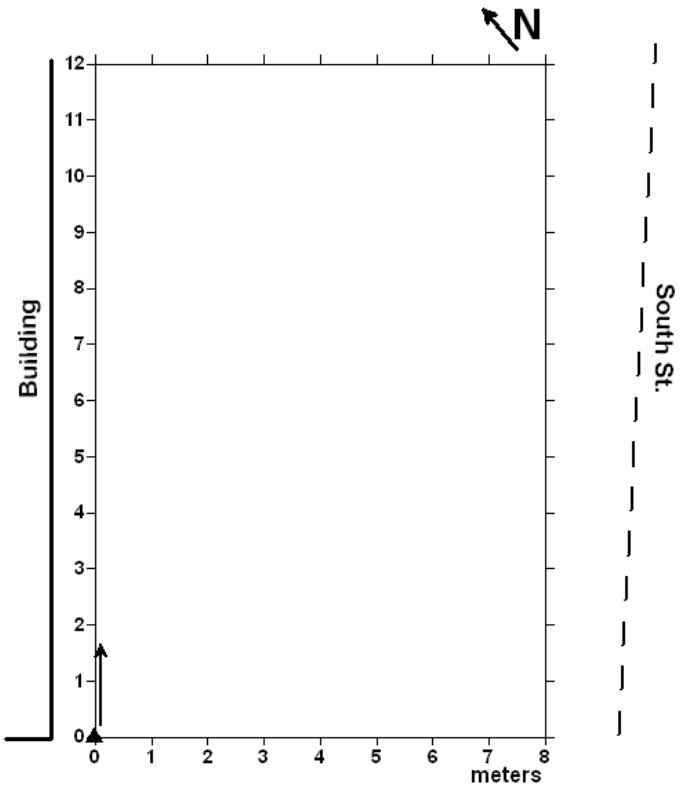

Figure 29: Sketch map of the GPR grid collected in the front concrete area at Kaka’ako Fire Station. The surveying direction is noted.

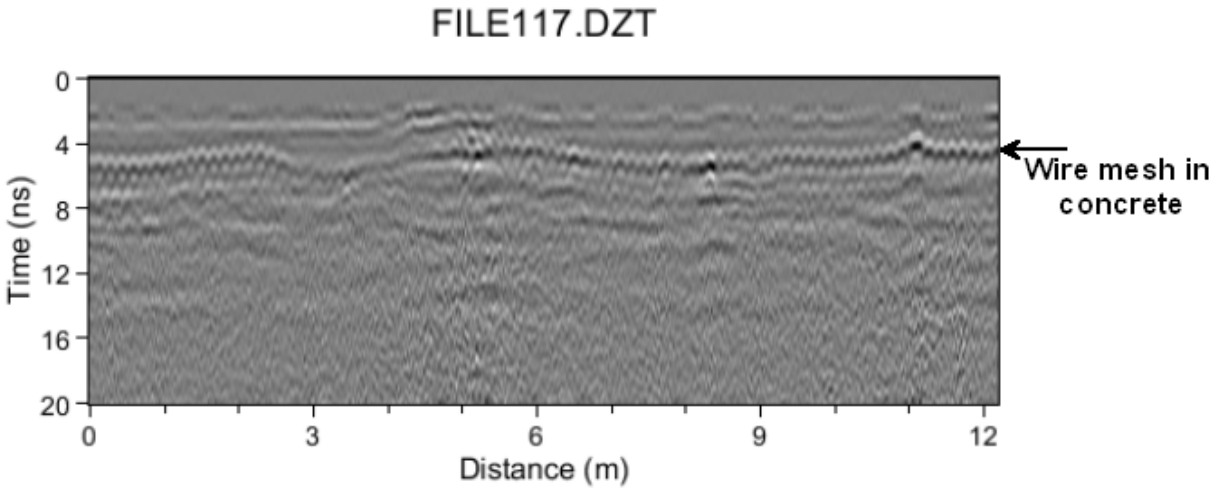

Figure 30: Reflection profile from the 900 MHz antenna dataset showing the high resolution of wire meshing within the concrete. The maximum depth penetration achieved with this antenna was approximately 50 cm.

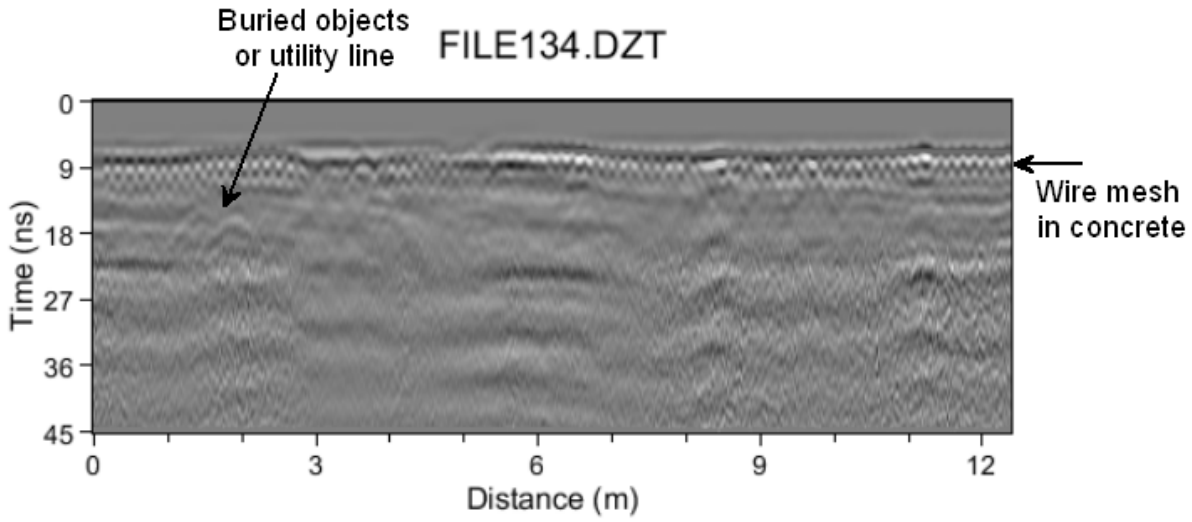

Figure 31: Reflection profile from the 400 MHz antenna dataset. The wire meshing within the concrete is clearly seen. Also seen is the reflection from a buried object or possible utility line. While likely not archaeologically significant, this shows that it is possible to resolve features below the wire mesh with this antenna frequency. The maximum depth penetration achieved with this antenna was about 1.3 meters.

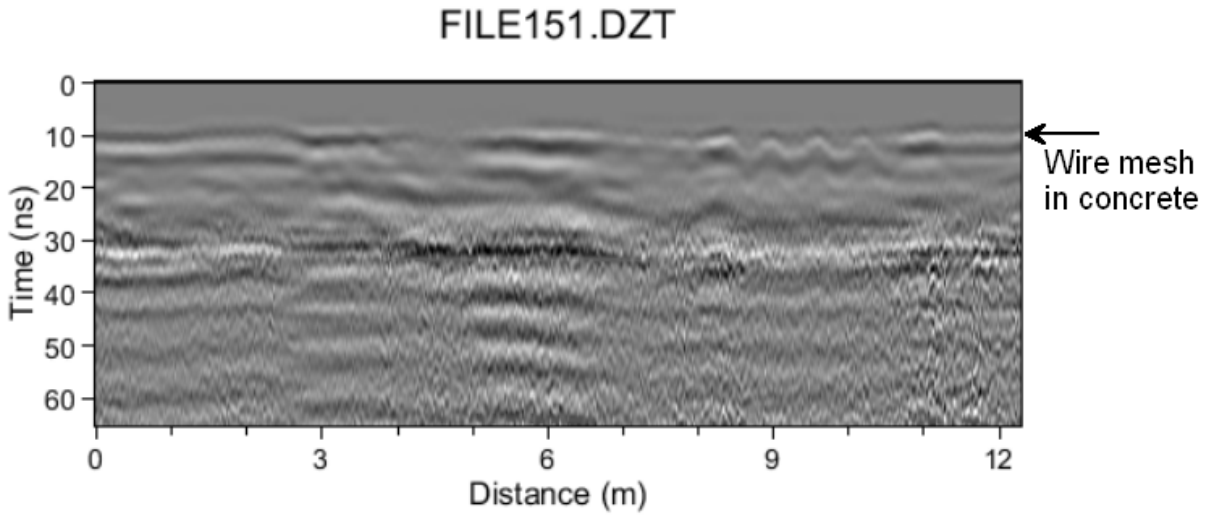

Figure 32: Reflection profile collected with the 270 MHz antenna. Only parts of the wire meshing are resolved with this antenna frequency, which are likely larger sections of rebar. The maximum depth penetration achieved with this antenna was approximately two meters.

Assessment and Recommendations

Based on these surveys, the overall potential for using the GPR method to map archaeological features and burials in this urban Honolulu setting is considered very good up to about 1.5 meters in depth. With this statement, however, should also come the clarification that imaging burials in this setting using GPR mapping is not necessarily a straight-forward task. As shown by the surveys conducted at the Alapai Transit Center and St. Augustine Church, many of the reflections related to known burials appear to relate to the burial shafts or stratigraphic disturbances from the sediments overlaying the burials, rather than the burials themselves. This is likely due to a number of factors, including the sediment mineralogy and deterioration of the burial and/or casket, if one exists. While these types of reflections are not always the most obvious in the GPR maps, it is considered encouraging that with careful data processing and analysis, it is possible to identify even subtle burials based on their surrounding disturbed sediments. More recent historic burials or burials with intact caskets appear to be a different case. As shown in the survey conducted in the back parking lot of the Kaka’ako Fire Station, which covers part of a known smallpox cemetery, historic burials appear as distinct, hyperbolic reflections in the GPR profiles, and particularly in the data collected with the 400 MHz antenna.

One of the most important goals of these surveys was to address the question of depth penetration and resolution. The maximum depths achieved with each antenna frequency at each location are summarized in Appendix A. While the 270 MHz antenna achieved the overall greatest depth at each location surveyed, this frequency was unable to resolve (or poorly resolve) some of the target features of interest, including some burials and other buried objects. It was, however, the most useful antenna for mapping larger, more deeply buried features such as utility lines. This was especially clear at the Kaka’ako Fire Station. The average depth penetration of the 400 MHz antenna ranged from approximately 1 to 1.5 meters, with good overall subsurface resolution. As shown in the stratigraphic and excavation information provided by CSH, a number of features, including burials, occur within about a meter in the ground in many of these areas. This makes the depth penetration achieved with the 400 MHz antenna adequate while still being able to clearly resolve the target features of interest. There is no question that the general sediments of these areas affect the overall transmission and reflection of the GPR energy. This is especially evident at the Civic Center Transit Station, where the hardened coral shelf layer corresponded exactly to the depth of energy attenuation with both the 400 MHz and 270 MHz antennas. Given these sedimentary constraints, and the minimal amount of extra depth penetration achieved with the 270 MHz in other areas, it is more important to consider the resolution of the features of interest. With features as small as burials, burial shafts, and historic debris, using an antenna that is able to resolve features as small as 10-15 cm (such as the 400 MHz) is likely a better solution than using an antenna that can propagate energy deeper. In contrast, the 900 MHz antenna provided the best resolution of features that occurred within about half a meter of the subsurface, which included wire meshing and some shallow buried objects. Energy attenuation beyond this depth, however, meant that many features deeper than about half a meter, including some burials, could not be imaged. The 900 MHz antenna is therefore not recommended for archaeological mapping in these areas, though it may have applicability in mapping shallow structural features, such as determining the presence of wire meshing as demonstrated in the concrete area of the Kaka’ako Fire Station.

In addition to antenna frequency, there are a number of collection and processing procedures that aided in the overall image generation, and thus interpretation, of the target features. Specific collection parameters used for each site are provided in Appendix B, but in general, a transect spacing of 50 cm or less was used in each of the grids, and a relatively high number of scans per meter (40) were collected to ensure high resolution slice-maps and reflection profiles could be generated. These are important parameters when using GPR mapping for archaeological applications such as this, as many of the features of interest in these areas were small or subtle, and would thus have been easily missed by using wide transect spacing or coarser resolution collection. The gains were also adjusted several times at each location until the best waveform was achieved (see Appendix B).

Post-acquisition data processing included the processing steps described in the "processing procedures" section above, as well as background noise filtering, which helps remove some of the extraneous noise from radio and cell phone transmissions, power lines, and other typical urban "clutter", as well as internal system noise. Finally, post-processing methods included range gaining, which amplifies subtler reflections, the use of small interpolation distances during slice-map generation, and applying smoothing filters. All of these post-processing methods are used for image enhancement and appearance only, and do not alter or modify the actual data.

Based on the information gathered from these surveys, it is recommended that future GPR mapping here be conducted with the 400 MHz antenna, with the possibility of using a 270 MHz for deeper utility mapping, or a 900 MHz for mapping shallower fill, wire mesh, or asphalt thickness. While the reflection profiles were overall more useful for identifying the shape, geometry, and depth of the reflections related to target features, it is recommended that profiles still be collected within grids. This ensures that each profile can be directly compared to the ones next to it, which directly assists in interpreting whether a reflection is being generated from a single object (such as a historic glass bottle), versus a burial or utility line (which would likely appear in two or more consecutive profiles). The slice-maps that can then be generated from collecting data in grids are often useful for determining the spatial extent of buried features and stratigraphic changes, both in plan view and according to depth. Amplitude slice-maps are also useful for mapping potential features that may exist in the reflection profiles but are not discernable to the human eye, as was the case with the possible utility lines mapped with the 270 MHz antenna at the Kaka'ako Fire Station. Finally, while these surveys were successful at mapping many features of interest, including several burials, many of the interpretations benefited greatly from the aid of subsurface and excavation information. It is therefore recommended that future GPR mapping be correlated with select trenching and excavation information wherever possible.

Conclusions

Six areas were surveyed with GPR mapping for this project to provide a representative sampling of the types of urban areas and features of interest that may be impacted by the Honolulu High-Capacity Transit Corridor Project (HHCTCP). The urban setting of this project in combination with the need for high-resolution mapping and depth analysis of the target features, which includes burials, made GPR mapping the most promising method for imaging these

features in a non-invasive way. By using three different antenna frequencies, a number of equipment parameters and collection procedures could be tested to evaluate the overall efficacy of this method in mapping the features of interest. Overall, this study was not only successful at determining that GPR mapping has use and potential for imaging buried features in this urban environment, but also demonstrated how the approach of testing a number of different parameters in a single study efficiently assessed if, how, and to what extent this imaging was possible.

References

Conyers, Lawrence B.

2004 *Ground-Penetrating Radar for Archaeology*. AltaMira Press, Walnut Creek, California.

2006 Ground-Penetrating Radar Techniques to Discover and Map Historic Graves. *Historical Archaeology* 40(3):64-73.

Conyers, Lawrence B. and Jeffrey E. Lucius

1996 Velocity Analysis in Archaeological Ground-Penetrating Radar Studies. *Archaeological Prospection* 3(1):25-38.

Pammer, Michelle F., Jon Tulchin, and Matt McDermott

2009 *Addendum to an Archaeological Inventory Survey and Cultural Impact Evaluation for the Alapai Transit Center and Joint Traffic Management Center Project, Honolulu Ahupua'a, Honolulu District, Island of Oah'u, TMK: (1) 2-1-042:004, 013*. Cultural Surveys Hawai‘i, Inc., October 2009.

Pfeffer, Michael T., Douglas Borthwick, and Hallett H. Hammatt

1993 An Archaeological Summaru of the Kaka‘ako Improvement District 1 Monitoring, Kaka‘ako, O‘ahu, Hawai‘i (TMKs 2-1-29 to 2-1-32, 2-1-46 to 2-1-48, 2-1-51, 2-1-54, and 2-1-55). Cultural Surveys Hawai‘i, Kailua, HI.

Yucha, Trevor M., Josephine M. Paolello, and Hallett H. Hammatt

2011 DRAFT Archaeological Inventory Survey for the St. Augustine-by-the-Sea Master Plan Project, Waikīkī Ahupua‘a, Honolulu (Kona) District, Island of O‘ahu, TMK [1] 2-6-26:012 & 015. Cultural Surveys Hawai‘i, Kailua, HI.

Appendix A: RDP, velocity, and maximum depth penetration achieved with each antenna frequency by location.

	Alapai	St. Augustine	Civic Center	Halekauwila Street	Fire Station Parking Lot/Smallpox Cemetery	Fire Station Front/Concrete Area
RDP	17.1	16.4	18.5	10.5	12	9
Velocity (cm/ns)	3.6	3.7	3.5	4.5	4	5
Max. Depth with 270 MHz (meters)	1.05	1.1	1.5	1.65	2.25	2
Max. Depth with 400 MHz (meters)	.9	1	1.2	1.55	1.75	1.3
Max. Depth with 900 MHz (meters)	.5	.5	.45	.55	.7	.5

Appendix B: Collection parameters for each antenna frequency by location.

Alapai

	Time window (ns)	Scans/meter	Filters	Gains	Transect spacing (meters)
270 MHz	65	40	HP: 135; LP: 540	-15, 2, 34, 34, 39	.5
400 MHz	40	40	HP: 200; LP: 800	-6, -6, 36, 36, 36	.5
900 MHz	20	40	HP: 450; LP: 1800	21, 21, 33, 42, 43	.25

St. Augustine

	Time window (ns)	Scans/meter	Filters	Gains	Transect spacing (meters)
270 MHz	65	40	HP: 135; LP: 540	-14, 2, 47, 52, 53	N/A
400 MHz	40	40	HP: 200; LP: 800	-8, 1, 45, 45, 45	N/A
900 MHz	20	40	HP: 450; LP: 1800	17, 18, 47, 51, 52	N/A

Civic Center

	Time window (ns)	Scans/meter	Filters	Gains	Transect spacing (meters)
270 MHz	65	40	HP: 135; LP: 540	-4, -4, 34, 34, 41	.5
400 MHz	40	40	HP: 200; LP: 800	-6, 2, 34, 36, 36	.5
900 MHz	20	40	HP: 450; LP: 1800	17, 17, 47, 47, 50	.25

Halekauwila Street

	Time window	Scans/meter	Filters	Gains	Transect spacing